MODELING YIELDS AT THE ZERO LOWER BOUND: ARE SHADOW RATES THE SOLUTION?

Jens H. E. Christensen and Glenn D. Rudebusch
Federal Reserve Bank of San Francisco, San Francisco, CA, USA

ABSTRACT

Recent U.S. Treasury yields have been constrained to some extent by the zero lower bound (ZLB) on nominal interest rates. Therefore, we compare the performance of a standard affine Gaussian dynamic term structure model (DTSM), which ignores the ZLB, to a shadow-rate DTSM, which respects the ZLB. Near the ZLB, we find notable declines in the forecast accuracy of the standard model, while the shadow-rate model forecasts well. However, 10-year yield term premiums are broadly similar across the two models. Finally, in applying the shadow-rate model, we find no gain from estimating a slightly positive lower bound on U.S. yields.

Keywords: Term structure modeling; zero lower bound; monetary policy

JEL classifications: G12; E43; E52; E58

Dynamic Factor Models
Advances in Econometrics, Volume 35, 75–125

ISSN: 0731-9053/doi:10.1108/S0731-905320150000035003

1. INTRODUCTION

With recent historic lows reached by nominal yields on government debt in several countries, understanding how to model the yield curve when some interest rates are near their zero lower bound (ZLB) is an issue that commands attention both for bond portfolio pricing and risk management and for macroeconomic and monetary policy analysis. Unfortunately, the workhorse representation in finance for bond pricing – the affine Gaussian dynamic term structure model – ignores the ZLB and places positive probabilities on negative interest rates. In essence, this model disregards the existence of a readily available zero-yield currency that an investor always has the option of holding and that dominates any security with a negative yield. This theoretical flaw in the standard model casts doubt on its usefulness for answering a key empirical question of this paper: how to best extract reliable market-based measures of expectations for future monetary policy when nominal interest rates are near the ZLB. Of course, as recent events have shown, at times, the ZLB can be a somewhat soft floor, and the non-negligible costs of transacting in and holding large amounts of currency have allowed government bond yields to push a bit below zero in several countries, notably Denmark and Switzerland. In our analysis below, we do not rigidly enforce a lower constraint of exactly zero on yields, but as a convenient abbreviation, we will refer to an episode of near-zero short rates as a ZLB period. The timing of this period for the United States is evident from the nominal U.S. Treasury zero-coupon yields shown in Fig. 1. The start of the ZLB period is commonly dated to December 16, 2008, when the Federal Open Market Committee (FOMC) lowered its target policy rate – the overnight federal funds rate – to a range from 0 to 1/4 percent, and it continued past the end of our sample in October 2014.

The past term structure literature offers three established frameworks to model yields near the ZLB that guarantee positive interest rates: stochastic-volatility models with square-root processes, Gaussian quadratic models, and Gaussian shadow-rate models. However, the first two of these approaches treat the ZLB as a reflecting barrier and not as an absorbing state, which seems inconsistent with the prolonged period of very low interest rates shown in Fig. 1. In contrast, shadow-rate models are completely consistent with an absorbing ZLB state for yields. In addition to these established frameworks, there is a growing literature offering new and interesting ways of accounting for the ZLB, including Filipović, Larsson, and Trolle (2014) and Monfort, Pegoraro, Renne, and Roussellet (2014).

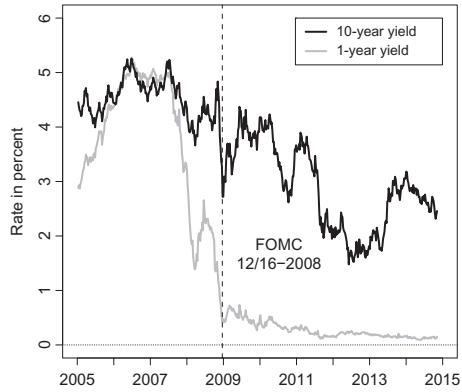

Fig. 1. Treasury Yields Since 2005. *Notes*: One- and 10-year weekly U.S. Treasury zero-coupon bond yields from January 7, 2005, to October 31, 2014.

While we consider all of these modeling approaches to be worthy of further investigation, Gaussian shadow-rate models are of particular interest because away from the ZLB they reduce exactly to standard Gaussian affine models. Therefore, the voluminous literature on affine Gaussian models remains completely applicable and relevant when given a modest shadow-rate tweak to handle the ZLB as we demonstrate. There have also been a few studies comparing the performance of these frameworks. For example, Kim and Singleton (2012) and Andreasen and Meldrum (2014) provide empirical results favoring shadow-rate representations over quadratic models. However, one important issue still requiring supporting evidence is the relative performance of the standard Gaussian affine dynamic term structure model (DTSM) versus an equivalent shadow-rate model. The standard affine DTSM is extremely well entrenched in the literature. It is both very popular and well understood. Despite its theoretical flaw noted above, could it be good enough for empirical purposes? To shed light on this issue, we compare the performance of a standard Gaussian DTSM of U.S. Treasury yields and its exact equivalent shadow-rate version. This comparison provides a clean read on the relative merits of standard and shadow-rate models during an episode of near-zero nominal yields.

For our comparative empirical analysis, we employ affine and shadow-rate versions of the arbitrage-free Nelson−Siegel (AFNS) model class that are estimated on the same data sample. The AFNS modeling structure provides an ideal framework for our analysis because of its excellent empirical properties and tractable and robust estimation.[1] For the Gaussian affine

model, we use the structure identified by Christensen and Rudebusch (2012) (henceforth CR), which is referred to throughout as the CR model. Since CR only detail the model's favorable properties through 2010, our analysis provides an update through October 2014, which includes a much longer ZLB period. As for the shadow-rate model, we use the shadow-rate AFNS model class introduced in Christensen and Rudebusch (2015). This is a latent-factor model in which the state variables have standard Gaussian dynamics, but the short rate is given an interpretation of a shadow rate in the spirit of Black (1995) to respect the ZLB for bond pricing. Christensen and Rudebusch (2015) apply this structure to a sample of near-ZLB Japanese government bond yields; however, they limit their analysis to the full-sample estimated parameters and state variables. Instead, we exploit the empirical tractability of that shadow-rate AFNS model, denoted here as the B-CR model, to study real-time forecast performance.[2]

Therefore, in this paper, we combine and extend the analysis of two recent papers. We compare the results from the CR model to those obtained from the B-CR model using the same sample of U.S. Treasury yield data. We can compare model performance across normal and ZLB periods and study real-time forecast performance, short-rate projections, term premium decompositions, and the properties of its estimated parameters. We find that the B-CR model provides slightly better fit as measured by in-sample metrics such as the RMSEs of fitted yields and the quasi likelihood values. Still, it is evident that a standard three-factor Gaussian DTSM like the CR model has enough flexibility to fit the cross-section of yields fairly well at each point in time even when the short end of the yield curve is flattened by the ZLB. However, it is not the case that the Gaussian model can account for all aspects of the term structure at the ZLB. Indeed, we show that the CR model clearly fails along two dimensions. First, despite fitting the yield curve, the model cannot capture the dynamics of yields at the ZLB. One stark indication of this is the high probability the model assigns to negative future short rates – obviously a poor prediction. Second, it misses the compression of yield volatility that occurs at the ZLB as expected future short rates are pinned near zero, longer-term rates fluctuate less. The B-CR model, even without incorporating stochastic volatility, can capture this effect. In terms of forecasting future short rates, we establish that the CR model is competitive over the normal period from 1995 to 2008. Thus, this model could have been expected to continue to perform well in the most recent period, if only it had not been for the problems associated with the ZLB. However, we also show that during the most recent period the B-CR model stands out in terms of forecasting future short rates in addition to performing on par with the regular model during the

normal period. Overall, a shadow-rate model shows clear empirical advantages. Still, the affine model may be a good first approximation for certain tasks. For example, we estimate 10-year term premiums that are broadly similar across the affine and shadow-rate models.

In addition, we study two empirical questions pertaining to the implementation of shadow-rate models. The first concerns the appropriate choice of the lower bound on yields. We argue that U.S. Treasury yield data point to zero as the appropriate lower bound, but throughout the paper, we consider the case with the lower bound treated as a free parameter that is determined by quasi maximum likelihood.[3] Our findings suggest that there are few if any gains in forecast performance from estimating the lower bound, and those gains come at the cost of fairly large estimated values of the lower bound. Since the estimated path of the shadow rate is sensitive to this choice (as we demonstrate), this is not an innocent parameter and should be chosen with care.[4] The second question we address is the closeness of the estimated parameters between a standard DTSM and its equivalent shadow-rate representation. If any differences between the parameter sets are small economically and statistically, this would provide a quick and efficient shortcut to avoid having to estimate shadow-rate models. Instead, one could simply rely on the estimated parameters from the matching standard model.[5] Unfortunately, we find that the differences in the estimated parameters can be sizable and economically important. Thus, while we cannot endorse the approach of relying on estimated parameters from a standard model as a way of implementing the corresponding shadow-rate model, our results still suggest that its optimal parameters do provide a reasonable guess of where to start the parameter optimization in the estimation of the shadow-rate model.

The rest of the paper is structured as follows. Section 2 describes Gaussian models in general as well as the CR model that we consider, while Section 3 details our shadow-rate model. Section 4 contains our empirical findings and discusses the implications for assessing policy expectations and term premiums in the current low-yield environment. Section 5 concludes. Three appendices contain additional technical details.

2. A STANDARD GAUSSIAN TERM STRUCTURE MODEL

In this section, we provide an overview of the affine Gaussian term structure model, which ignores the ZLB, and describe the CR model.

2.1. The General Model

Let $P_t(\tau)$ be the price of a zero-coupon bond at time t that pays \$ 1, at maturity $t+\tau$. Under standard assumptions, this price is given by

$$P_t(\tau) = E_t^P\left[\frac{M_{t+\tau}}{M_t}\right]$$

where the stochastic discount factor, M_t, denotes the value at time t_0 of a claim at a future date t, and the superscript P refers to the actual, or real-world, probability measure underlying the dynamics of M_t. (As we will discuss in the next section, there is no restriction in this standard setting to constrain $P_t(\tau)$ from rising above its par value; i.e., the ZLB is ignored.)

We follow the usual reduced-form empirical finance approach that models bond prices with unobservable (or latent) factors, here denoted as X_t, and the assumption of no residual arbitrage opportunities. We assume that X_t follows an affine Gaussian process with constant volatility, with dynamics in continuous time given by the solution to the following stochastic differential equation (SDE):

$$\mathrm{d}X_t = K^P\left(\theta^P - X_t\right)\mathrm{d}t + \Sigma \mathrm{d}W_t^P$$

where K^P is an $n \times n$ mean-reversion matrix, θ^P is an $n \times 1$ vector of mean levels, Σ is an $n \times n$ volatility matrix, and W_t^P is an n-dimensional Brownian motion. The dynamics of the stochastic discount function are given by

$$\mathrm{d}M_t = r_t M_t \mathrm{d}t + \Gamma_t' M_t \mathrm{d}W_t^P$$

and the instantaneous risk-free rate, r_t, is assumed affine in the state variables

$$r_t = \delta_0 + \delta_1' X_t$$

where $\delta_0 \in R$ and $\delta_1 \in R^n$. The risk premiums, Γ_t, are also affine as in Duffee (2002):

$$\Gamma_t = \gamma_0 + \gamma_1 X_t$$

where $\gamma_0 \in R^n$ and $\gamma_1 \in R^{n \times n}$.

Duffie and Kan (1996) show that these assumptions imply that zero-coupon yields are also affine in X_t:

$$y_t(\tau) = -\frac{1}{\tau}A(\tau) - \frac{1}{\tau}B(\tau)'X_t$$

where $A(\tau)$ and $B(\tau)$ are given as solutions to the following system of ordinary differential equations:

$$\frac{\mathrm{d}B(\tau)}{\mathrm{d}\tau} = -\delta_1 - \left(K^P + \Sigma\gamma_1\right)'B(\tau), \quad B(0) = 0,$$
$$\frac{\mathrm{d}A(\tau)}{\mathrm{d}\tau} = -\delta_0 + B(\tau)'\left(K^P\theta^P - \Sigma\gamma_0\right) + \frac{1}{2}\sum_{j=1}^{n}\left[\Sigma'B(\tau)B(\tau)'\Sigma\right]_{jj}, \quad A(0) = 0$$

Thus, the $A(\tau)$ and $B(\tau)$ functions are calculated *as if* the dynamics of the state variables had a constant drift term equal to $K^P\theta^P - \Sigma\gamma_0$ instead of the actual $K^P\theta^P$ and a mean-reversion matrix equal to $K^P + \Sigma\gamma_1$ as opposed to the actual K^P. The probability measure with these alternative dynamics is frequently referred to as the risk-neutral, or Q, probability measure since the expected return on any asset under this measure is equal to the risk-free rate r_t that a risk-neutral investor would demand. The difference is determined by the risk premium Γ_t and reflects investors' aversion to the risks embodied in X_t.

Finally, we define the term premium as

$$\mathrm{TP}_t(\tau) = y_t(\tau) - \frac{1}{\tau}\int_t^{t+\tau} E_t^P[r_s]\,\mathrm{d}s$$

That is, the term premium is the difference in expected return between a buy and hold strategy for a τ-year. Treasury bond and an instantaneous rollover strategy at the risk-free rate r_t.[6]

2.2. The CR Model

A wide variety of Gaussian term structure models have been estimated. Here, we describe the empirical representation identified by CR that uses

high-frequency observations on U.S. Treasury yields from a sample that includes the recent ZLB period. It improves the econometric identification of the latent factors, which facilitates model estimation.[7] The CR model is an AFNS representation as introduced in Christensen, Diebold, and Rudebusch (2011) with three latent state variables, $X_t = (L_t, S_t, C_t)$. These are described by the following system of SDEs under the risk-neutral Q-measure:[8]

$$\begin{pmatrix} \mathrm{d}L_t \\ \mathrm{d}S_t \\ \mathrm{d}C_t \end{pmatrix} = \begin{pmatrix} 0 & 0 & 0 \\ 0 & \lambda & -\lambda \\ 0 & 0 & \lambda \end{pmatrix} \left[\begin{pmatrix} \theta_1^Q \\ \theta_2^Q \\ \theta_3^Q \end{pmatrix} - \begin{pmatrix} L_t \\ S_t \\ C_t \end{pmatrix} \right] \mathrm{d}t + \Sigma \begin{pmatrix} \mathrm{d}W_t^{L,Q} \\ \mathrm{d}W_t^{S,Q} \\ \mathrm{d}W_t^{C,Q} \end{pmatrix}, \quad \lambda > 0 \quad (1)$$

where Σ is the constant covariance (or volatility) matrix.

In addition, the instantaneous risk-free rate is defined by

$$r_t = L_t + S_t \quad (2)$$

This specification implies that zero-coupon bond yields are given by

$$y_t(\tau) = L_t + \left(\frac{1 - \mathrm{e}^{-\lambda\tau}}{\lambda\tau} \right) S_t + \left(\frac{1 - \mathrm{e}^{-\lambda\tau}}{\lambda\tau} - \mathrm{e}^{-\lambda\tau} \right) C_t - \frac{A(\tau)}{\tau}$$

where the factor loadings in the yield function match the level, slope, and curvature loadings introduced in Nelson and Siegel (1987). The final yield-adjustment term, $A(\tau)/\tau$, captures convexity effects due to Jensen's inequality.

The model is completed with a risk premium specification that connects the factor dynamics to the dynamics under the real-world P-measure as explained in Section 2.1. The maximally flexible specification of the AFNS model has P-dynamics given by[9]

$$\begin{pmatrix} \mathrm{d}L_t \\ \mathrm{d}S_t \\ \mathrm{d}C_t \end{pmatrix} = \begin{pmatrix} \kappa_{11}^P & \kappa_{12}^P & \kappa_{13}^P \\ \kappa_{21}^P & \kappa_{22}^P & \kappa_{23}^P \\ \kappa_{31}^P & \kappa_{32}^P & \kappa_{33}^P \end{pmatrix} \left[\begin{pmatrix} \theta_1^P \\ \theta_2^P \\ \theta_3^P \end{pmatrix} - \begin{pmatrix} L_t \\ S_t \\ C_t \end{pmatrix} \right] \mathrm{d}t + \begin{pmatrix} \sigma_{11} & 0 & 0 \\ \sigma_{21} & \sigma_{22} & 0 \\ \sigma_{31} & \sigma_{32} & \sigma_{33} \end{pmatrix} \begin{pmatrix} \mathrm{d}W_t^{L,P} \\ \mathrm{d}W_t^{S,P} \\ \mathrm{d}W_t^{C,P} \end{pmatrix} \quad (3)$$

Using both in- and out-of-sample performance measures, CR went through a careful empirical analysis to justify various zero-value restrictions on the

K^P matrix. Imposing these restrictions results in the following dynamic system for the P-dynamics:

$$\begin{pmatrix} dL_t \\ dS_t \\ dC_t \end{pmatrix} = \begin{pmatrix} 10^{-7} & 0 & 0 \\ \kappa_{21}^P & \kappa_{22}^P & \kappa_{23}^P \\ 0 & 0 & \kappa_{33}^P \end{pmatrix} \left(\begin{pmatrix} 0 \\ \theta_2^P \\ \theta_3^P \end{pmatrix} - \begin{pmatrix} L_t \\ S_t \\ C_t \end{pmatrix} \right) dt + \Sigma \begin{pmatrix} dW_t^{L,P} \\ dW_t^{S,P} \\ dW_t^{C,P} \end{pmatrix} \quad (4)$$

where the covariance matrix Σ is assumed diagonal and constant. Note that in this specification, the Nelson−Siegel level factor is restricted to be an independent unit-root process under both probability measures.[10] As discussed in CR, this restriction helps improve forecast performance independent of the specification of the remaining elements of K^P. Because interest rates are highly persistent, empirical autoregressive models, including DTSMs, suffer from substantial small-sample estimation bias. Specifically, model estimates will generally be biased toward a dynamic system that displays much less persistence than the true process (so estimates of the real-world mean-reversion matrix, K^P, are upward biased). Furthermore, if the degree of interest rate persistence is underestimated, future short rates would be expected to revert to their mean too quickly causing their expected longer-term averages to be too stable. Therefore, the bias in the estimated dynamics distorts the decomposition of yields and contaminates estimates of long-maturity term premiums. As described in detail in Bauer, Rudebusch, and Wu (2012), bias-corrected K^P estimates are typically very close to a unit-root process, so we view the imposition of the unit-root restriction as a simple shortcut to overcome small-sample estimation bias.

We re-estimated this CR model over a larger sample of weekly nominal U.S. Treasury zero-coupon yields from January 4, 1985, until October 31, 2014, for eight maturities: three months, six months, one year, two years, three years, five years, seven years, and 10 years.[11] The model parameter estimates are reported in Table 1. As in CR, we test the significance of the four parameter restrictions imposed on K^P in the CR model relative to the unrestricted AFNS model.[12] The four parameter restrictions are not rejected by the data at conventional levels of significance similar to what CR report; thus, the CR model appears flexible enough to capture the relevant information in the data compared with an unrestricted model.

Table 1. Parameter Estimates for the CR Model.

K^P	$K^P_{\cdot,1}$	$K^P_{\cdot,2}$	$K^P_{\cdot,3}$	θ^P		Σ
$K^P_{1,\cdot}$	10^{-7}	0	0	0	σ_{11}	0.0066
						(0.0001)
$K^P_{2,\cdot}$	0.3390	0.4157	−0.4548	0.0218	σ_{22}	0.0100
	(0.1230)	(0.1154)	(0.0843)	(0.0244)		(0.0002)
$K^P_{3,\cdot}$	0	0	0.6189	−0.0247	σ_{33}	0.0271
			(0.1571)	(0.0074)		(0.0004)

Notes: The estimated parameters of the K^P matrix, θ^P vector, and diagonal Σ matrix are shown for the CR model. The estimated value of λ is 0.4482 (0.0022). The numbers in parentheses are the estimated parameter standard deviations. The maximum log likelihood value is 70,754.54.

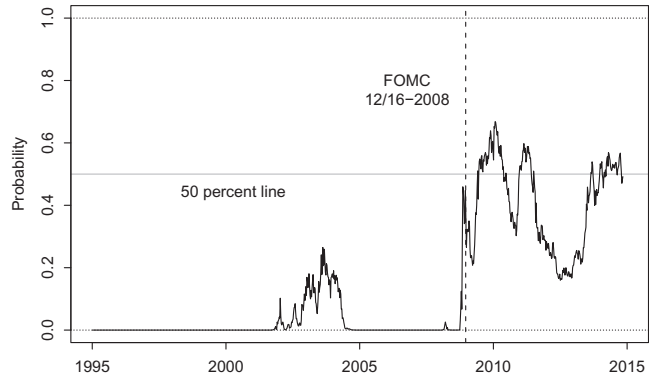

Fig. 2. Probability of Negative Short Rates. *Notes:* Illustration of the conditional probability of negative short rates three months ahead from the CR model.

2.3. Negative Short-Rate Projections in Standard Models

Before turning to the description of the shadow-rate model, it is useful to reinforce the basic motivation for our analysis by examining short-rate forecasts from the estimated CR model. With regard to short-rate forecasts, any standard affine Gaussian DTSM may place positive probabilities on future negative interest rates. Accordingly, Fig. 2 shows the probability that the short rate three months out will be negative obtained from rolling real-time weekly re-estimations of the CR model. Prior to 2008 the probabilities of future negative interest rates are negligible except for a brief period in 2003 and 2004 when the Fed's policy rate temporarily stood at 1 percent. However, near the ZLB – since late 2008 – the model is typically

predicting substantial likelihoods of impossible realizations. Worse still, whenever these probabilities are above 50 percent (indicated with a solid gray horizontal line), the model's conditional expected short rate is negative, which has frequently been the case since 2009.

3. A SHADOW-RATE MODEL

In this section, we describe an option-based approach to the shadow-rate model and estimate a shadow-rate analog to the CR model with U.S. data.

3.1. The Option-Based Approach to the Shadow-Rate Model

The concept of a shadow interest rate as a modeling tool to account for the ZLB can be attributed to Black (1995). He noted that the observed nominal short rate will be nonnegative because currency is a readily available asset to investors that carries a nominal interest rate of zero. Therefore, the existence of currency sets a ZLB on yields. To account for this ZLB, Black postulated a shadow short rate, s_t, that is unconstrained by the ZLB. The usual observed instantaneous risk-free rate, r_t, which is used for discounting cash flows when valuing securities, is then given by the greater of the shadow rate or zero:

$$r_t = \max\{0, s_t\} \tag{5}$$

Accordingly, as s_t falls below zero, the observed r_t simply remains at the zero bound.

While Black (1995) described circumstances under which the zero bound on nominal yields might be relevant, he did not provide specifics for implementation. The small set of empirical research on shadow-rate models has relied on numerical methods for pricing.[13] To overcome the computational burden of numerical-based estimation that limits the use of shadow-rate models, Krippner (2013) suggested an alternative option-based approach that makes shadow-rate models almost as easy to estimate as the standard model.[14] To illustrate this approach, consider two bond-pricing situations: one without currency as an alternative asset, and the other that has a currency in circulation with a constant nominal value and no transaction costs. In the world without currency, the price of a shadow-rate zero-coupon bond, $P_t(\tau)$, may trade above par; that is, its risk-neutral expected

instantaneous return equals the risk-free shadow short rate, which may be negative. In contrast, in the world with currency, the price at time t for a zero-coupon bond that pays 1 when it matures in τ years is given by $\underline{P}_t(\tau)$. This price will never rise above par, so nonnegative yields will never be observed.

Now consider the relationship between the two bond prices at time t for the shortest (say, overnight) maturity available, δ. In the presence of currency, investors can either buy the zero-coupon bond at price $P_t(\delta)$ and receive one unit of currency the following day or just hold the currency. As a consequence, this bond price, which would equal the shadow bond price, must be capped at 1:

$$\begin{aligned}\underline{P}_t(\delta) &= \min\{1, P_t(\delta)\} \\ &= P_t(\delta) - \max\{P_t(\delta) - 1, 0\}\end{aligned}$$

That is, the availability of currency implies that the overnight claim has a value equal to the zero-coupon shadow bond price minus the value of a call option on the zero-coupon shadow bond with a strike price of 1. More generally, we can express the price of a bond in the presence of currency as the price of a shadow bond minus the call option on values of the bond above par:

$$\underline{P}_t(\tau) = P_t(\tau) - C_t^A(\tau, \tau; 1)$$

where $C_t^A(\tau, \tau; 1)$ is the value of an American call option at time t with maturity in τ years and strike price 1 written on the shadow bond maturing in τ years. In essence, in a world with currency, the bond investor has had to sell off the possible gain from the bond rising above par at any time prior to maturity.

Unfortunately, analytically valuing this American option is complicated by the difficulty in determining the early exercise premium. However, Krippner (2013) argues that there is an analytically close approximation based on tractable European options. Specifically, Krippner (2013) shows that the ZLB instantaneous forward rate, $\underline{f}_t(\tau)$, is

$$\underline{f}_t(\tau) = f_t(\tau) + z_t(\tau)$$

where $f_t(\tau)$ is the instantaneous forward rate on the shadow bond, which may go negative, while $z_t(\tau)$ is an add-on term given by

$$z_t(\tau) = \lim_{\delta \to 0} \left[\frac{\partial}{\partial \delta} \frac{C_t^E(\tau, \tau + \delta; 1)}{P_t(\tau + \delta)} \right] \tag{6}$$

where $C_t^E(\tau, \tau + \delta; 1)$ is the value of a European call option at time t with maturity $t + \tau$ and strike price 1 written on the shadow discount bond maturing at $t + \tau + \delta$. Thus, the observed yield-to-maturity is

$$\begin{aligned} \underline{y}_t(\tau) &= \frac{1}{\tau} \int_t^{t+\tau} \underline{f}_t(s) \mathrm{d}s \\ &= \frac{1}{\tau} \int_t^{t+\tau} f_t(s) \mathrm{d}s + \frac{1}{\tau} \int_t^{t+\tau} \lim_{\delta \to 0} \left[\frac{\partial}{\partial \delta} \frac{C_t^E(s, s + \delta; 1)}{P_t(s + \delta)} \right] \mathrm{d}s \\ &= y_t(\tau) + \frac{1}{\tau} \int_t^{t+\tau} \lim_{\delta \to 0} \left[\frac{\partial}{\partial \delta} \frac{C_t^E(s, s + \delta; 1)}{P_t(s + \delta)} \right] \mathrm{d}s \end{aligned}$$

Hence, bond yields constrained at the ZLB can be viewed as the sum of the yield on the unconstrained shadow bond, denoted $y_t(\tau)$, which is modeled using standard tools, and an add-on correction term derived from the price formula for the option written on the shadow bond that provides an upward push to deliver the higher nonnegative yields actually observed.

As highlighted by Christensen and Rudebusch (2015), the Krippner (2013) framework should be viewed as not fully internally consistent and simply an approximation to an arbitrage-free model.[15] Of course, away from the ZLB, with a negligible call option, the model will match the standard arbitrage-free term structure representation. In addition, the size of the approximation error near the ZLB has been determined via simulation for Japanese yield data in Christensen and Rudebusch (2015) to be quite modest, and we provide similar evidence in Appendix A for our sample of U.S. Treasury yields.

3.2. The B-CR Model

In theory, the option-based shadow-rate result is quite general and applies to any assumptions made about the dynamics of the shadow-rate process. However, as implementation requires the calculation of the limit in Eq. (6), the option-based shadow-rate models are limited practically to the

Gaussian model class. The AFNS class is well suited for this extension.[16] In the shadow-rate AFNS model, the shadow risk-free rate is defined as the sum of level and slope as in Eq. (2) in the original AFNS model class, while the affine short rate is replaced by the nonnegativity constraint:

$$s_t = L_t + S_t, \quad r_t = \max\{0, s_t\}$$

All other elements of the model remain the same. Namely, the dynamics of the state variables used for pricing under the Q-measure remain as described in Eq. (1), so the yield on the shadow discount bond maintains the popular Nelson and Siegel (1987) factor loading structure

$$y_t(\tau) = L_t + \left(\frac{1-e^{-\lambda\tau}}{\lambda\tau}\right)S_t + \left(\frac{1-e^{-\lambda\tau}}{\lambda\tau} - e^{-\lambda\tau}\right)C_t - \frac{A(\tau)}{\tau}$$

where $A(\tau)/\tau$ is the same maturity-dependent yield-adjustment term.

The corresponding instantaneous shadow forward rate is given by

$$f_t(\tau) = -\frac{\partial}{\partial T}\ln P_t(\tau) = L_t + e^{-\lambda\tau}S_t + \lambda\tau e^{-\lambda\tau}C_t + A^f(\tau)$$

where the yield-adjustment term in the instantaneous forward rate function is given by

$$\begin{aligned}
A^f(\tau) &= -\frac{\partial A(\tau)}{\partial\tau} \\
&= -\frac{1}{2}\sigma_{11}^2\tau^2 - \frac{1}{2}\left(\sigma_{21}^2+\sigma_{22}^2\right)\left(\frac{1-e^{-\lambda\tau}}{\lambda}\right)^2 \\
&\quad -\frac{1}{2}\left(\sigma_{31}^2+\sigma_{32}^2+\sigma_{33}^2\right)\left[\frac{1}{\lambda^2} - \frac{2}{\lambda^2}e^{-\lambda\tau} - \frac{2}{\lambda}\tau e^{-\lambda\tau} + \frac{1}{\lambda^2}e^{-2\lambda\tau} + \frac{2}{\lambda}\tau e^{-2\lambda\tau} + \tau^2 e^{-2\lambda\tau}\right] \\
&\quad -\sigma_{11}\sigma_{21}\tau\frac{1-e^{-\lambda\tau}}{\lambda} - \sigma_{11}\sigma_{31}\left[\frac{1}{\lambda}\tau - \frac{1}{\lambda}\tau e^{-\lambda\tau} - \tau^2 e^{-\lambda\tau}\right] \\
&\quad -\left(\sigma_{21}\sigma_{31}+\sigma_{22}\sigma_{32}\right)\left[\frac{1}{\lambda^2} - \frac{2}{\lambda^2}e^{-\lambda\tau} - \frac{1}{\lambda}\tau e^{-\lambda\tau} + \frac{1}{\lambda^2}e^{-2\lambda\tau} + \frac{1}{\lambda}\tau e^{-2\lambda\tau}\right]
\end{aligned}$$

Krippner (2013) provides a formula for the ZLB instantaneous forward rate, $\underline{f}_t(\tau)$, that applies to any Gaussian model

$$\underline{f}_t(\tau) = f_t(\tau)\Phi\left(\frac{f_t(\tau)}{\omega(\tau)}\right) + \omega(\tau)\frac{1}{\sqrt{2\pi}}\exp\left(-\frac{1}{2}\left[\frac{f_t(\tau)}{\omega(\tau)}\right]^2\right)$$

where $\Phi(\cdot)$ is the cumulative probability function for the standard normal distribution, $f_t(\tau)$ is the shadow forward rate, and $\omega(\tau)$ is related to the conditional variance, $v(\tau, \tau+\delta)$, appearing in the shadow bond option price formula as follows:

$$\omega(\tau)^2 = \frac{1}{2}\lim_{\delta \to 0}\frac{\partial^2 v(\tau, \tau+\delta)}{\partial \delta^2}$$

Within the shadow-rate AFNS model, $\omega(\tau)$ takes the following form:

$$\begin{aligned}\omega(\tau)^2 = {} & \sigma_{11}^2\tau + \left(\sigma_{21}^2 + \sigma_{22}^2\right)\frac{1-\mathrm{e}^{-2\lambda\tau}}{2\lambda} \\ & + \left(\sigma_{31}^2 + \sigma_{32}^2 + \sigma_{33}^2\right)\left[\frac{1-\mathrm{e}^{-2\lambda\tau}}{4\lambda} - \frac{1}{2}\tau\mathrm{e}^{-2\lambda\tau} - \frac{1}{2}\lambda\tau^2\mathrm{e}^{-2\lambda\tau}\right] \\ & + 2\sigma_{11}\sigma_{21}\frac{1-\mathrm{e}^{-\lambda\tau}}{\lambda} + 2\sigma_{11}\sigma_{31}\left[-\tau\mathrm{e}^{-\lambda\tau} + \frac{1-\mathrm{e}^{-\lambda\tau}}{\lambda}\right] \\ & + \left(\sigma_{21}\sigma_{31} + \sigma_{22}\sigma_{32}\right)\left[-\tau\mathrm{e}^{-2\lambda\tau} + \frac{1-\mathrm{e}^{-2\lambda\tau}}{2\lambda}\right]\end{aligned}$$

Therefore, the zero-coupon bond yields that observe the ZLB, denoted $\underline{y}_t(\tau)$, are easily calculated as

$$\underline{y}_t(\tau) = \frac{1}{\tau}\int_t^{t+\tau}\left[f_t(s)\Phi\left(\frac{f_t(s)}{\omega(s)}\right) + \omega(s)\frac{1}{\sqrt{2\pi}}\exp\left(-\frac{1}{2}\left[\frac{f_t(s)}{\omega(s)}\right]^2\right)\right]\mathrm{d}s$$

Table 2. Parameter Estimates for the B-CR Model.

K^P	$K^P_{\cdot,1}$	$K^P_{\cdot,2}$	$K^P_{\cdot,3}$	θ^P		Σ
$K^P_{1,\cdot}$	10^{-7}	0	0	0	σ_{11}	0.0069
						(0.0001)
$K^P_{2,\cdot}$	0.1953	0.3138	−0.4271	0.0014	σ_{22}	0.0112
	(0.1474)	(0.1337)	(0.0904)	(0.0364)		(0.0002)
$K^P_{3,\cdot}$	0	0	0.4915	−0.0252	σ_{33}	0.0257
			(0.1200)	(0.0087)		(0.0004)

Notes: The estimated parameters of the K^P matrix, θ^P vector, and diagonal Σ matrix are shown for the B-CR model. The estimated value of λ is 0.4700 (0.0026). The numbers in parentheses are the estimated parameter standard deviations. The maximum log likelihood value is 71,408.90.

As in the affine AFNS model, the shadow-rate AFNS model is completed by specifying the price of risk using the essentially affine risk premium specification introduced by Duffee (2002), so the real-world dynamics of the state variables can be expressed as in Eq. (3). Again, in an unrestricted case, both K^P and θ^P are allowed to vary freely relative to their counterparts under the Q-measure. However, we focus on the case with the same K^P and θ^P restrictions as in the CR model, that is, the P-dynamics are given by Eq. (4), on the assumption that outside of the ZLB period, the shadow-rate model would properly collapse to the standard CR form. We label this shadow-rate model as the B-CR model as already discussed in Section 1.

We estimate the B-CR model from January 4, 1985, until October 31, 2014, for eight maturities: three months, six months, one year, two years, three years, five years, seven years, and 10 years.[17] The estimated B-CR model parameters are reported in Table 2. Later on, we make a more comprehensive analysis of the estimated parameters in both models. For now, as with the CR model, we test the significance of the four parameter restrictions imposed on K^P in the B-CR model relative to the unrestricted B-AFNS model.[18] Fig. 3 shows that, for most sample cutoff points since 1995, the four parameter restrictions are not rejected by the data at conventional levels of significance. Also shown with a solid gray line are the quasi likelihood ratio tests of the six restrictions in the most parsimonious B-AFNS model with independent factors relative to the unrestricted B-AFNS model, which are clearly rejected. Thus, similar to the CR model, the B-CR model appears flexible enough to capture the relevant information in the data compared with an unrestricted model.

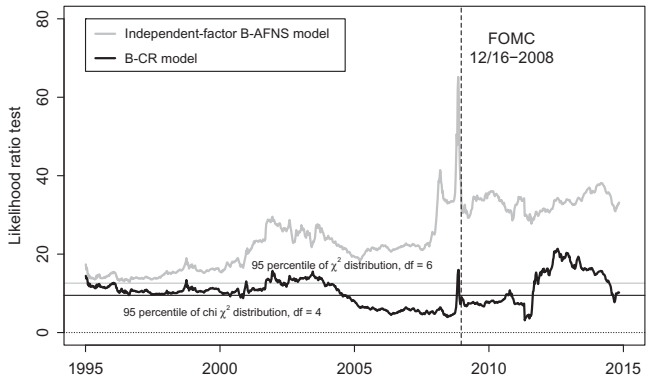

Fig. 3. Quasi Likelihood Ratio Tests of Parameter Restrictions in B-AFNS Models. *Notes:* Illustration of the value of quasi likelihood ratio tests of the restrictions imposed in the independent-factor B-AFNS model, and in the B-AFNS model underlying the B-CR model, relative to the B-AFNS model with unrestricted K^P-matrix and diagonal Σ-matrix. The analysis covers weekly re-estimations from January 6, 1995, to October 31, 2014, a total of 1,035 observations, while the full data set used in the analysis covers the period from January 4, 1985, to October 31, 2014.

3.3. Measuring the Effect of the ZLB

To provide evidence that we should anticipate to see at least some difference across the regular and shadow-rate models, we turn our focus to the value of the option to hold currency, which we define as the difference between the yields that observe the ZLB and the comparable lower shadow discount bond yields that do not. Fig. 4 shows these yield spreads at the 5- and 10-year maturity based on real-time rolling weekly re-estimations of the B-CR model starting in 1995 through October 31, 2014. Beyond a very few temporary small spikes, the option had economically insignificant value prior to the failure of Lehman Brothers in the fall of 2008.[19] However, despite the zero short rate since 2008, it is not really until after August 2011 that the option obtains significant sustained value. At its peak in the fall of 2012, the yield spread was 80 and 60 basis points at the five- and 10-year maturity, respectively. Option values at those levels suggest that it should matter for model performance whether a model accounts for the ZLB of nominal yields. Section 4 is dedicated to analyzing this question, but first we discuss the choice of lower bound in the shadow-rate model.

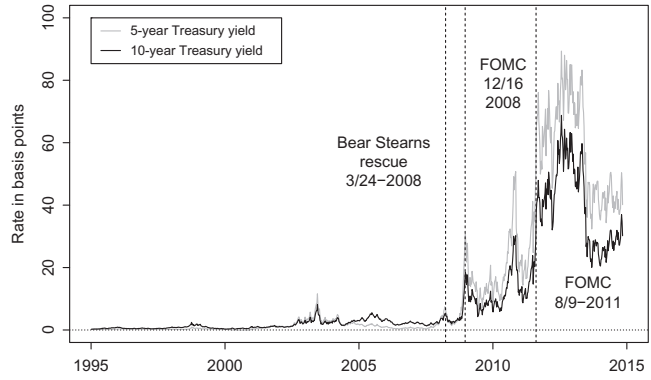

Fig. 4. Value of Option to Hold Currency. *Notes:* We show time-series plots of the value of the option to hold currency embedded in the Treasury yield curve as estimated in real time by the B-CR model. The data cover the period from January 6, 1995, to October 31, 2014.

3.4. Nonzero Lower Bound for the Short Rate

In this section, we consider a generalization of the B-CR model that allows for the lower bound of the short rate to differ from zero, that is,

$$r_t = \max\{r_{\min}, s_t\}$$

Christensen and Rudebusch (2015) provide the formula for the forward rate that respects the $r_{\min}$ lower bound:[20]

$$\underline{f}_t(\tau) = r_{\min} + (f_t(\tau) - r_{\min})\Phi\left(\frac{f_t(\tau) - r_{\min}}{\omega(\tau)}\right) + \omega(\tau)\frac{1}{\sqrt{2\pi}}\exp\left(-\frac{1}{2}\left[\frac{f_t(\tau) - r_{\min}}{\omega(\tau)}\right]^2\right)$$

where the shadow forward rate, $f_t(\tau)$, and $\omega(\tau)$ remain as before.

A few papers have used a nonzero lower bound for the short rate. In the case of U.S. Treasury yields, Wu and Xia (2014) simply fix the lower bound at 25 basis points. A similar approach applied to Japanese, U.K., and U.S. yields is followed by Ichiue and Ueno (2013).[21] As an alternative, Kim and Priebsch (2013) leave $r_{\min}$ as a free parameter to be determined in the model estimation. Using U.S. Treasury yields they report an estimated value of 14 basis points.

In theory, the lower bound should be zero because that is the nominal return on holding currency, which is a readily available alternative to holding bonds. Furthermore, U.S. Treasury yield data also supports a choice of zero for the lower bound. Specifically, in the daily H.15 database through October 31, 2014 (of which we use a weekly subsample), the zero boundary is *never* violated. The one-month yield is 0 on 51 dates, the three-month yield is 0 on 8 dates, while the six-month yield never goes below 2 basis points. In addition, since late 2008, the spread between the six- and three-month yields is always nonnegative with a single exception, October 11, 2013, when it was negative 1 basis point. Thus, with three- and six-month yields less than 10 basis points and the yield curve steep for much of the time spent near the ZLB, the choice of zero for the lower bound of the short rate appears to be a reasonable assumption that is supported by both the data and theoretical considerations.[22] Still, it is econometrically feasible to leave $r_{\min}$ as a free parameter to be determined by the data as in Kim and Priebsch (2013). Thus, ultimately, it is an empirical question what is the appropriate choice for the lower bound of the short rate in shadow-rate models. To make a comprehensive and in-depth assessment of the economical and statistical importance of this parameter, we use rolling weekly re-estimations of the B-CR model with and without restricting $r_{\min}$ to zero.

Fig. 5 illustrates the estimated value of $r_{\min}$ from the rolling re-estimations since January 6, 1995. At the start of this sample, $r_{\min}$ was estimated to be almost 285 basis points, but since then, it has been trending lower. As of October 31, 2014, the full-sample estimate of the lower bound was 11 basis points. Even that relatively low value of $r_{\min}$ censors much of the variation in the short end of the yield curve. There are 215 weekly observations of the three-month yield below that level in our sample, while the corresponding number for the six-month and one-year yields is 124 and 8, respectively. Given that we have 307 weekly observations from the ZLB period (defined as the period since December 19, 2008), more than 70 percent of the time spent in the ZLB period the model would ignore variation in the three-month yields, while it ignores variation in the six-month yield more than 40 percent of the time.

In Fig. 5(b), we show quasi likelihood ratio tests of restricting $r_{\min}$ to zero in the B-CR model relative to leaving it unrestricted. We note that the zero restriction has been systematically rejected since 1995. Most problematically, the rejection is strongest since 2010 when a lower bound of zero appears to be most appropriate according to the level of short-term yields in the data. Thus, the need to fully understand the effects of varying the lower bound in shadow-rate models is evident.

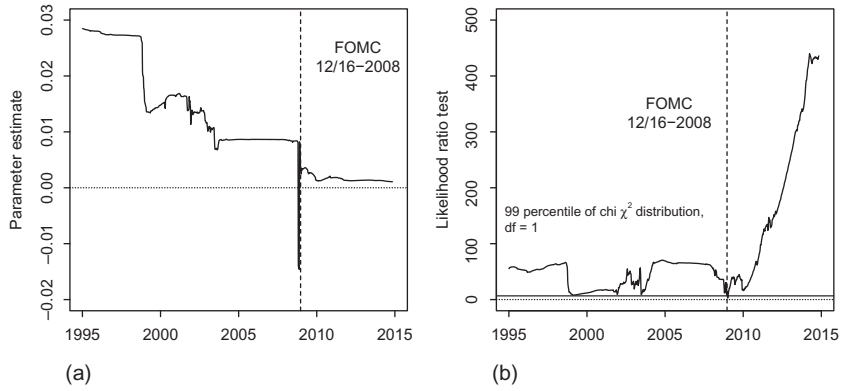

Fig. 5. Estimates of $r_{\min}$ and Quasi Likelihood Ratio Tests of its Zero Restriction. *Notes:* Panel (a) illustrates the estimated value of $r_{\min}$ in the B-CR model from weekly re-estimations from January 6, 1995, to October 31, 2014, a total of 1,035 observations. Panel (b) shows quasi likelihood ratio tests of restricting $r_{\min}$ to zero in the B-CR model, also based on weekly re-estimations from January 6, 1995, to October 31, 2014. The full data set used in the analysis covers the period from January 4, 1985, to October 31, 2014.

To demonstrate that the choice of $r_{\min}$ may not be innocuous, consider the estimated shadow-rate path. Fig. 6 shows this path for the B-CR model with and without restricting $r_{\min}$ to zero. For comparison, the estimated short-rate path from the CR model is also shown. All three models are indistinguishable along this dimension before 2008, so the figure only shows the estimated paths since then. Note that the estimated shadow-rate path is sensitive to the choice of $r_{\min}$, as was also highlighted by Bauer and Rudebusch (2014). For this reason, our results below will include B-CR model specifications with $r_{\min}$ restricted to zero and freely estimated.

4. COMPARING AFFINE AND SHADOW-RATE MODELS

In this section, we compare the empirical affine and shadow-rate models across a variety of dimensions, including parameter stability, in-sample fit, volatility dynamics, and out-of-sample forecast performance.

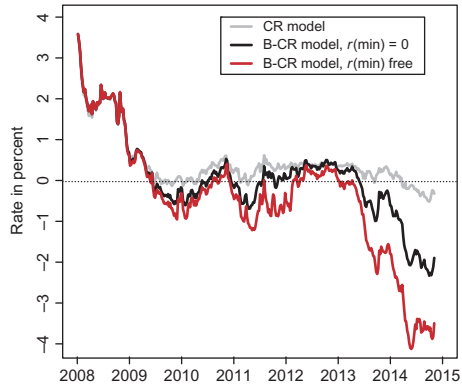

Fig. 6. Estimated Short- and Shadow-Rate Paths. *Notes:* Illustration of the estimated shadow-rate paths from the B-CR model with and without restricting $r_{\min}$ to zero with a comparison to the estimated short-rate path from the CR model. All three paths are based on full sample estimations with data covering the period from January 4, 1985, to October 31, 2014.

4.1. Analysis of Parameter Estimates

To begin, we analyze the parameter stability and similarity of the empirical affine and shadow-rate models, where the latter is estimated with and without restricting $r_{\min}$ to zero throughout. We also assess the reasonableness of using estimated parameters from the affine model in combination with the shadow-rate model as a way of avoiding the burden of making a full shadow-rate model estimation.

Fig. 7 shows the estimated parameters in the mean-reversion matrix K^P. First, we note that all three models give very similar parameter estimates before December 2008. This is not surprising since the shadow-rate models collapse to the affine model away from the lower bound, and it does not matter much whether the lower bound is fixed at zero or left as a free parameter. Second, since late 2008, we do see some larger deviations with a tendency for the shadow-rate models to produce higher persistence of the slope and curvature factors as indicated by their lower estimates of κ^P_{22} and κ^P_{33}. However, judged by the estimated parameter standard deviations reported in Tables 1 and 2, these differences in the individual parameters do not appear to be statistically significant.

In Fig. 8, we compare the estimated volatility parameters. While the estimated volatility parameters for the level factor are fairly similar across all

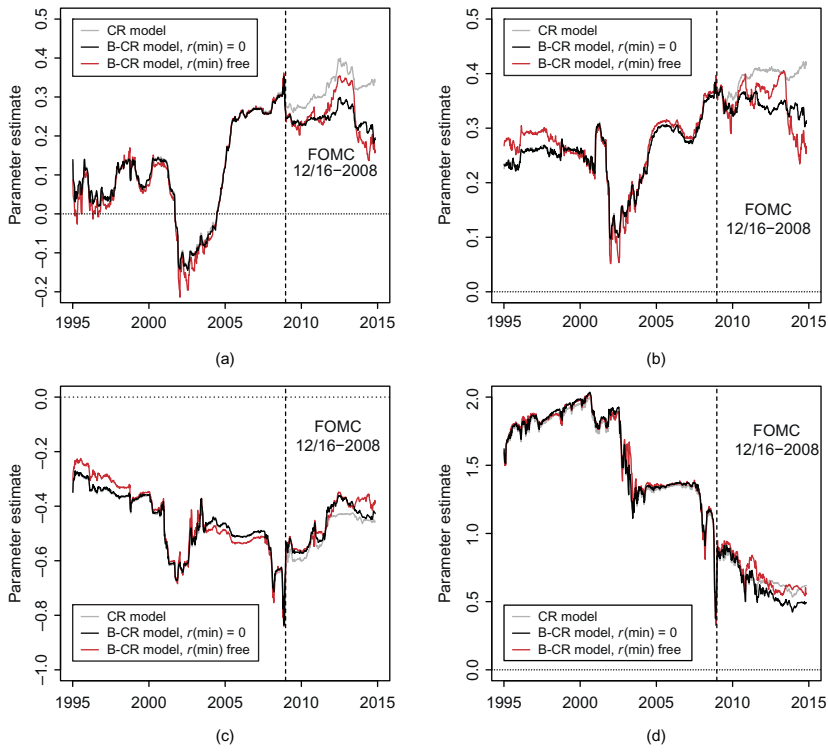

Fig. 7. Estimates of Mean-Reversion Parameters. *Notes:* Illustration of the estimated parameters in the mean-reversion K^P matrix in the CR and B-CR models, where the latter is estimated with and without restricting $r_{\min}$ to zero. The analysis covers weekly re-estimations from January 6, 1995, to October 31, 2014, a total of 1,035 observations, while the full data set used covers the period from January 4, 1985, to October 31, 2014. Estimates of (a) κ^P_{21}; (b) κ^P_{22}; (c) κ^P_{23}; and (d) κ^P_{33}.

three models throughout the entire period as can be seen in Fig. 8(a), there are larger differences in the estimated volatility of the slope and curvature factors during the most recent period as illustrated in Fig. 8(b) and (c). In the shadow-rate models, the slope factor is allowed to be more volatile in the post-crisis period compared to the standard model as it is not required to fully match the low volatility of short-term yields near the ZLB whenever the shadow rate is in negative territory.

Fig. 9 shows the estimated mean parameters since 1995. These parameters represent another area where the models "learn" something about

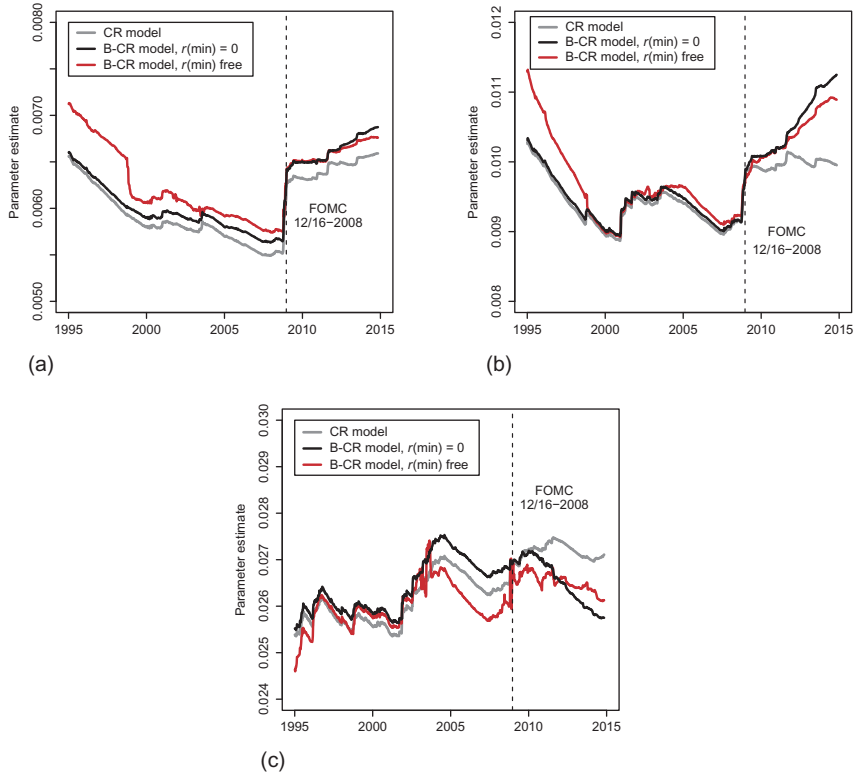

Fig. 8. Estimates of Volatility Parameters. *Notes:* Illustration of the estimated parameters in the volatility Σ matrix in the CR and B-CR models, where the latter is estimated with and without restricting $r_{\min}$ to zero. The analysis covers weekly re-estimations from January 6, 1995, to October 31, 2014, a total of 1,035 observations, while the full data set used covers the period from January 4, 1985, to October 31, 2014. Estimates of (a) σ_{11}; (b) σ_{22}; and (c) σ_{33}.

the true parameter values through the updating during the ZLB period. The low yield levels in this period translate into gradually declining estimates of the mean parameters, θ_2^P and θ_3^P, in particular the estimate of θ_3^P has declined notably since the crisis. Since the curvature factor in its role as the stochastic mean of the slope factor represents expectations for future monetary policy, a potential explanation for the decline in its estimated mean would be the anchoring of monetary policy expectations in the

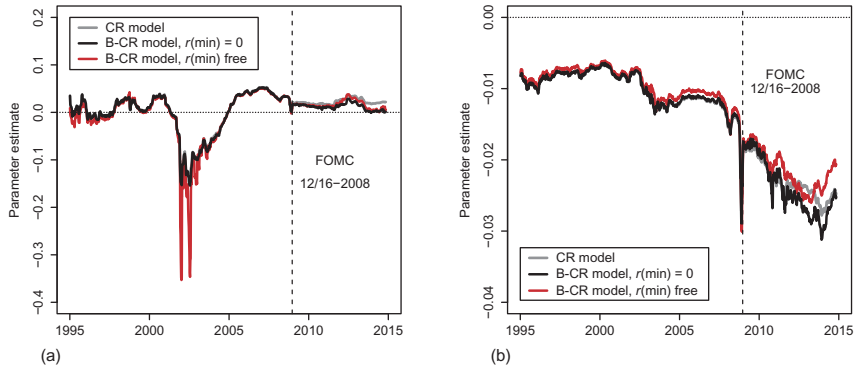

Fig. 9. Estimates of Mean Parameters. *Notes:* Illustration of the estimated parameters in the mean θ^P vector in the CR and B-CR models, where the latter is estimated with and without restricting $r_{\min}$ to zero. The analysis covers weekly re-estimations from January 6, 1995, to October 31, 2014, a total of 1,035 observations, while the full data set used covers the period from January 4, 1985, to October 31, 2014. Estimates of (a) θ_2^P and (b) θ_3^P.

medium term at a low level, perhaps reflecting various forms of policy forward guidance employed by the FOMC since late 2008.

Finally, in Fig. 10, we compare the various estimates of the λ parameter that determines the rate of decay in the yield factor loading of the slope factor and the peak maturity in the yield factor loading of the curvature factor. Here, we see a more long-term trend toward lower values. This suggests that investors' speculation about future monetary policy as represented through the variation of the curvature factor has tended to take place at longer maturities more recently than compared to two decades ago. What role the greater transparency of the FOMC's monetary policy decisions plays for this trend is an interesting question that we leave for future research.

To summarize our findings so far, overall, the differences between the standard and the shadow-rate models for individual parameters look relatively small and are in most cases not statistically significant. Still, it could be the case that the minor differences combined could add up to material differences not only statistically, but also economically. We end the section by analyzing this important question further.

The way we proceed is to take the estimated parameters from the B-CR model with $r_{\min}$ restricted to zero as of December 28, 2007, and those from the CR model as of December 28, 2007, and October 31, 2014. We then

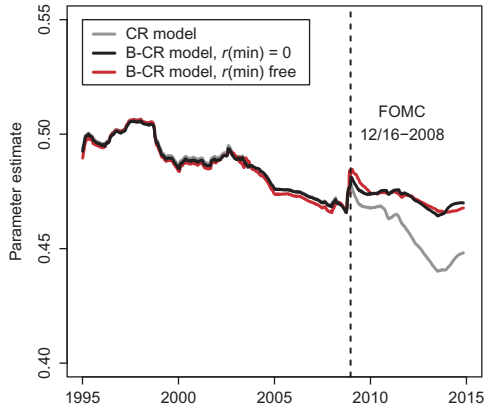

Fig. 10. Estimates of the λ Parameter. *Notes:* Illustration of the estimated λ parameter in the CR and B-CR models, where the latter is estimated with and without restricting $r_{\min}$ to zero. The analysis covers weekly re-estimations from January 6, 1995, to October 31, 2014, a total of 1,035 observations, while the full data set used covers the period from January 4, 1985, to October 31, 2014.

combine these three parameter vectors with the B-CR model with $r_{\min}$ restricted to zero to obtain the corresponding filtered state variables as of October 31, 2014. Finally, we use each pair of parameters and filtered state variables to calculate the projection of the short rate as of October 31, 2014. These projected paths are shown in Fig. 11. The benchmark in the comparison is obtained by using the B-CR model's own estimated parameters as of October 31, 2014, to filter the state variables on that date and combine them to generate the associated short-rate projection as of October 31, 2014, shown with a solid black line in Fig. 11.

It is immediately noted that the differences in the short-rate projections are huge. The parameters estimated with the CR and B-CR models as of December 28, 2007, both imply a rather quick rate of mean reversion *and* to a high-level approaching 4 percent in the long run, while the parameters estimated with the CR model as of October 31, 2014, imply an even quicker rate of mean reversion at first, but they have the short-rate leveling off near 3 percent in the long run due to lower estimated values of the mean parameters, θ_2^P and θ_3^P. In contrast, the B-CR model's own projection implies a later liftoff, a more gradual normalization of monetary policy, and to a lower long-run level of about 2 percent, due to the higher persistence (lower κ_{22}^P and κ_{33}^P estimates) and lower means of the slope and curvature factors relative to the two alternative parameter vectors.

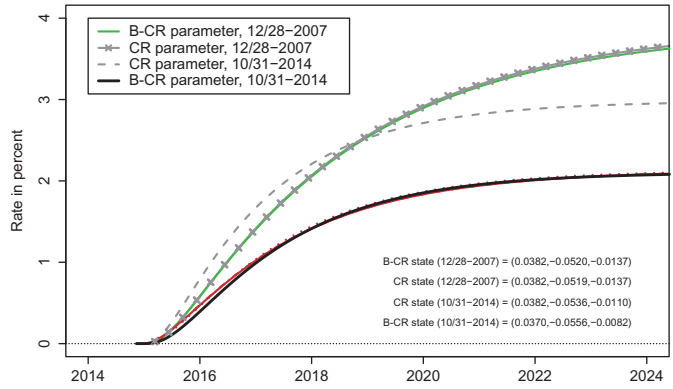

Fig. 11. Sensitivity of Short-Rate Projections to Model Parameters. *Notes:* Illustration of short-rate projections as of October 31, 2014, implied by the B-CR model with $r_{\min}$ restricted to zero using different model parameters and state variables as explained in the main text.

To shed more light on the source of the disagreement about the short-rate paths, in the lower right corner of Fig. 11, we report the four different filtered state variable vectors used as conditioning variables in the calculations of the short-rate projections. We note that they are slightly different from one another. However, to demonstrate that this is not the cause for the differences in the short-rate projections, we condition on all four state variable vectors using the B-CR model with its estimated parameters as of October 31, 2014. In addition to the solid black line, this produces the dotted gray lines in the figure, which are practically indistinguishable from the solid black line. Thus, the variation in the short-rate projections in Fig. 11 is entirely driven by differences in the parameter vectors.

Furthermore, we note that the differences are material, not just economically, but also statistically. The log likelihood values obtained from evaluating the extended Kalman filter of the B-CR model at each of the four parameter sets are 71,200.19, 71,181.75, 71,260.51, and 71,408.90, respectively, where the latter is the value of the likelihood function of the B-CR model evaluated at its own optimal parameters as of October 31, 2014. Thus, the deviations in each parameter do combine into huge likelihood differences as well.

Based on these findings we cannot recommend using pre-crisis parameter estimates to assess recent policy expectations as done in Bauer and Rudebusch (2014), and even the use of contemporaneous parameter

estimates from the affine model in combination with the shadow-rate model does not seem warranted as a way to alleviate the burden of estimation. To facilitate the estimation of the shadow-rate model, we feel that, at most, what can be gained from estimating the matching affine model is to use its optimal parameters as a starting point for the parameter optimization in the estimation of the shadow-rate model.

Finally, we note that these results demonstrate the importance of undertaking rolling real-time model estimations like the ones performed in this paper when evaluating model performance near the ZLB. However, it remains an open question to what extent the state variables will maintain their recent high persistence or revert back toward the lower pre-crisis levels once the normalization of policy rates begins. Thus, we caution that there is a risk that rolling estimations might underperform during the early stages of the subsequent policy tightening cycle.

4.2. In-Sample Fit and Yield Volatility

The summary statistics of the fit to yield levels of the affine and shadow-rate models are reported in Table 3. They indicate a very similar fit in the normal period up until the end of 2008. However, since then, we see a notable advantage to the shadow-rate models that is also reflected in the likelihood values. Still, we conclude from this in-sample analysis that it is not in the model fit that the shadow-rate model really distinguishes itself from its regular cousin, and this conclusion is not sensitive to the choice of lower bound.

However, a serious limitation of standard Gaussian models is the assumption of constant yield volatility, which is particularly unrealistic when periods of normal volatility are combined with periods in which yields are greatly constrained in their movements near the ZLB. A shadow-rate model approach can mitigate this failing significantly. In the CR model, where zero-coupon yields are affine functions of the state variables, model-implied conditional predicted yield volatilities are given by the square root of

$$V_t^P\left[y_T^N(\tau)\right] = \frac{1}{\tau^2} B(\tau)' V_t^P[X_T] B(\tau)$$

where $T-t$ is the prediction period, τ is the yield maturity, $B(\tau)$ contains the yield factor loadings, and $V_t^P[X_T]$ is the conditional covariance matrix of the state variables.[23] In the B-CR model, on the other hand,

Table 3. Summary Statistics of the Fitted Errors.

RMSE	Maturity in Months								All Yields
	3	6	12	24	36	60	84	120	
Full sample									
CR	30.82	15.02	0.00	2.49	0.00	3.05	2.71	10.74	12.81
B-CR, $r_{\min} = 0$	29.89	14.27	0.90	2.26	0.27	2.67	2.28	9.97	12.32
B-CR, $r_{\min}$ free	29.78	14.23	0.88	2.23	0.35	2.65	2.36	9.86	12.27
Normal period (Jan. 6, 1995–Dec. 12, 2008)									
CR	32.76	15.66	0.00	2.51	0.00	3.01	2.50	10.53	13.47
B-CR, $r_{\min} = 0$	32.69	15.48	0.74	2.39	0.09	2.80	2.09	10.48	13.40
B-CR, $r_{\min}$ free	32.69	15.49	0.62	2.40	0.10	2.81	2.16	10.50	13.41
ZLB period (Dec. 19, 2008–Oct. 31, 2014)									
CR	21.13	12.05	0.00	2.42	0.00	3.17	3.41	11.56	10.07
B-CR, $r_{\min} = 0$	13.40	7.55	1.37	1.64	0.57	2.06	2.93	7.60	6.96
B-CR, $r_{\min}$ free	12.11	7.04	1.54	1.30	0.75	1.91	3.02	6.60	6.27

Notes: Shown are the root-mean-squared fitted errors (RMSEs) for the CR and B-CR models, where the latter is estimated with and without restricting $r_{\min}$ to zero. All numbers are measured in basis points. The data covers the period from January 6, 1985, to October 31, 2014.

zero-coupon yields are nonlinear functions of the state variables and conditional predicted yield volatilities have to be generated by standard Monte Carlo simulation. Fig. 12 shows the implied three-month conditional yield volatility of the three-month and two-year yields from the CR and B-CR models.

To evaluate the fit of these predicted three-month-ahead conditional yield standard deviations, they are compared to a standard measure of realized volatility based on the same data used in the model estimation, but at daily frequency. The realized standard deviation of the daily changes in the interest rates are generated for the 91-day period ahead on a rolling basis. The realized variance measure is used by Andersen and Benzoni (2010), Collin-Dufresne, Goldstein, and Jones (2009), as well as Jacobs and Karoui (2009) in their assessments of stochastic volatility models. For each observation date t the number of trading days N during the subsequent 91-day time window is determined and the realized standard deviation is calculated as

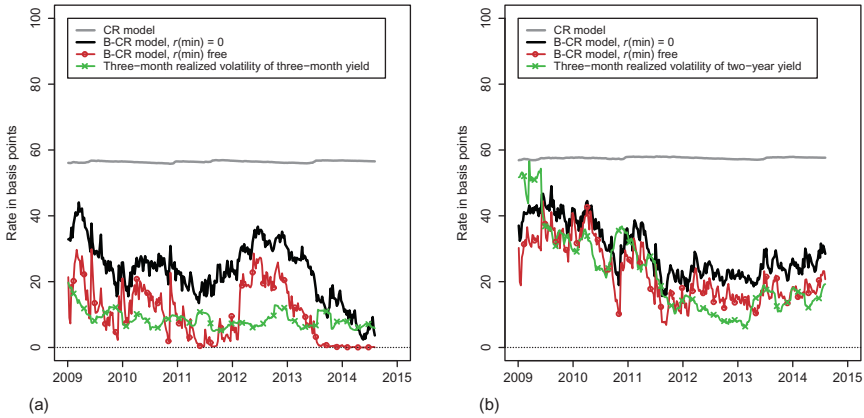

Fig. 12. Three-Month Conditional Yield Volatilities Since 2009. *Notes:* Panel (a) illustrates the three-month conditional volatility of the three-month yield implied by the estimated CR and B-CR models, where the latter is estimated with $r_{\min}$ both restricted to zero and left free. Also shown is the subsequent three-month realized volatility of the three-month yield based on daily data. Panel (b) illustrates the corresponding results for the three-month conditional volatility of the two-year yield.

$$RV_{t,\tau}^{\text{STD}} = \sqrt{\sum_{n=1}^{N} \Delta y_{t+n}^2(\tau)}$$

where $\Delta y_{t+n}(\tau)$ is the change in yield $y(\tau)$ from trading day $t+(n-1)$ to trading day $t+n$.[24]

While the conditional yield volatility from the CR model changes little (merely reflecting the updating of estimated parameters), the conditional yield volatility from the B-CR models fairly closely matches the realized volatility series.[25] As for leaving $r_{\min}$ as a free parameter, we note that it does lead to a slightly closer fit to the realized yield volatilities of medium-term yields, but it comes at the tradeoff of periodically producing effectively zero volatility of short-term yields as shown in Fig. 12(a).

4.3. Forecast Performance

In this section, we first compare the ability of standard and shadow-rate models to forecast future short rates, before we proceed to evaluate their ability to forecast the entire cross section of yields.

4.3.1. Short-Rate Forecasts

Extracting the term premiums embedded in the Treasury yield curve is ultimately an exercise in generating accurate policy rate expectations. Thus, to study bond investors' expectations in real time, we use the rolling re-estimations of the CR model and its shadow-rate equivalents on expanding samples – adding one week of observations each time, a total of 1,035 estimations. As a result, the end dates of the expanding samples range from January 6, 1995, to October 31, 2014. For each end date during that period, we project the short-rate six months, one year, and two years ahead.[26] Importantly, the estimates of these objects rely essentially only on information that was available in real time. Besides examining the full sample, we also distinguish between forecast performance in the normal period prior to the policy rate reaching its effective lower bound (the 13 years from 1995 through 2008) and the ZLB period.

For robustness, we include results from another established U.S. Treasury term structure model introduced in Kim and Wright (2005), henceforth KW), which is a standard latent three-factor Gaussian term structure model of the kind described in Section 2.1.[27] Summary statistics for the forecast errors relative to the subsequent realizations of the target overnight federal funds rate set by the FOMC are reported in Table 4, which also contains the forecast errors obtained using a random walk assumption. We note the strong forecast performance of the KW model relative to the CR model during the normal period, while it is equally obvious that the KW model underperforms grossly during the ZLB period since December 19, 2008. As expected, the CR and B-CR models exhibit fairly similar performance during the normal period, while the B-CR model stands out in the most recent ZLB period. Importantly, we note that, for forecasting future short rates near the ZLB, forecast accuracy is not improved by allowing for a nonzero lower bound in the B-CR model despite the reported in-sample statistical advantage of doing so.

Fig. 13 compares the models' one-year-ahead forecasts to the subsequent target rate realizations. The KW model's systematic overprediction of future target rates since late 2008 stands out. For the CR model, the deterioration in forecast performance is not really detectable until after the August 2011 FOMC meeting when explicit forward guidance was first introduced. Since the CR model mitigates finite-sample bias in the estimates of the mean-reversion matrix K^P by imposing a unit-root property on the Nelson–Siegel level factor, it suggests that the recent deterioration for the CR model must be caused by other more fundamental factors. Importantly, though, the shadow-rate models appear much less affected by any such issues.

Table 4. Summary Statistics for Target Federal Funds Rate Forecast Errors.

	Six-Month Forecast		One-Year Forecast		Two-Year Forecast	
	Mean	RMSE	Mean	RMSE	Mean	RMSE
Full forecast period						
Random walk	14.94	80.01	30.16	142.74	60.58	232.35
KW model	7.44	62.61	51.42	124.46	125.38	222.64
CR model	−0.51	63.27	13.99	123.55	55.01	224.25
B-CR model, $r_{\min} = 0$	3.51	59.79	21.80	117.95	64.79	216.53
B-CR model, $r_{\min}$ free	10.16	57.58	29.22	116.86	72.80	213.76
Normal forecast period						
Random walk	20.71	94.19	40.73	165.87	77.47	262.75
KW model	−3.40	69.68	35.62	132.67	102.34	226.36
CR model	−0.33	72.08	16.41	141.20	57.30	250.94
B-CR model, $r_{\min} = 0$	2.57	69.97	24.00	136.56	69.30	243.18
B-CR model, $r_{\min}$ free	9.45	67.07	31.45	134.89	75.99	239.22
ZLB forecast period						
Random walk	0.00	0.00	0.00	0.00	0.00	0.00
KW model	35.53	38.70	96.53	97.28	207.99	208.73
CR model	−0.97	30.17	7.08	43.93	46.82	69.37
B-CR model, $r_{\min} = 0$	5.95	12.35	15.51	19.91	48.62	54.32
B-CR model, $r_{\min}$ free	11.98	15.79	22.87	26.47	61.37	65.82

Notes: Summary statistics of the forecast errors—mean and root-mean-squared errors (RMSEs)—of the target overnight federal funds rate six months, one year, and two years ahead. The forecasts are weekly. The top panel covers the full forecast period that starts on January 6, 1995, and runs until May 2, 2014, for the six-month forecasts (1,009 forecasts), until November 1, 2013, for the one-year forecasts (983 forecasts), and until November 2, 2012, for the two-year forecasts (931 forecasts). The middle panel coves the normal forecast period from January 6, 1995, to December 12, 2008, 728 forecasts. The lower panel covers the zero lower bound forecast period that starts on December 19, 2008, and runs until May 2, 2014, for the six-month forecasts (281 forecasts), until November 1, 2013, for the one-year forecasts (255 forecasts), and until November 2, 2012, for the two-year forecasts (203 forecasts). All measurements are expressed in basis points.

4.3.2. Yield Forecasts

Now, we extend the analysis above and evaluate the models' yield forecast performance more broadly. Note that, due to the nonlinear yield function in the shadow-rate models, their yield forecasts are generated using Monte Carlo simulations. Also, we note that yield forecasts from the KW model are not available and therefore not included in the analysis.

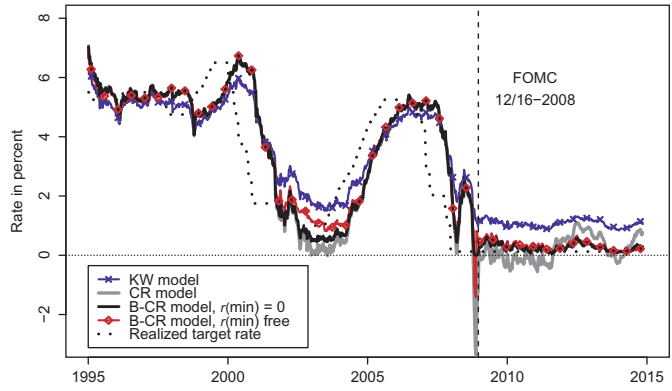

Fig. 13. Forecasts of the Target Overnight Federal Funds Rate. *Notes:* Forecasts of the target overnight federal funds rate one year ahead from the CR and B-CR models, where the latter is estimated with $r_{\min}$ both restricted to zero and left free. Also shown are the corresponding forecasts from the KW model. Subsequent realizations of the target overnight federal funds rate are included, so at date t, the figure shows forecasts as of time t and the realization from t plus one year. The forecast data are weekly observations from January 6, 1995, to October 31, 2014.

Table 5 reports the summary statistics of errors for real-time forecasts of three-month, two-year, five-year, and 10-year Treasury yields during the normal period from January 6, 1995, to December 12, 2008. First, we note that there is barely any difference in the shadow-rate models between restricting $r_{\min}$ to zero or leaving it free during the normal period. Second, in this period, the CR model is slightly worse at forecasting short- and medium-term yields than the B-CR model, but has a slight advantage at forecasting long-term yields. Finally, we note that the CR and B-CR models are competitive at forecasting yields of all maturities up to one year ahead relative to the random walk.

Table 6 reports the summary statistics of yield forecast errors during the recent ZLB period for the same four yield maturities considered in Table 5. First, because all three models have mean-reverting factor dynamics for the slope and curvature factors, they systematically underestimate how long yields would remain low in the aftermath of the financial crisis. This aspect of the data clearly benefits the random walk assumption. Second, the B-CR model dominates at forecasting short-term yields consistent with its ability to forecast future federal funds target rates reported in Table 4. On the other hand, the CR model continues to exhibit a strong performance at forecasting long-term yields. Finally, it is again the case that leaving $r_{\min}$ as a free parameter when

Table 5. Summary Statistics for Forecast Errors of U.S. Treasury Yields in the Normal Period.

	Six-Month Forecast		One-Year Forecast		Two-Year Forecast	
	Mean	RMSE	Mean	RMSE	Mean	RMSE
Three-month yield						
Random walk	−20.19	90.14	−39.28	157.11	−75.03	248.91
CR model	−29.27	89.51	−46.30	154.19	−86.86	254.06
B-CR model, $r_{\min} = 0$	−32.53	88.39	−53.73	151.32	−97.88	248.24
B-CR model, $r_{\min}$ free	−37.60	87.83	−59.48	150.69	−103.06	245.26
Two-year yield						
Random walk	−20.14	86.68	−36.74	132.02	−73.05	207.26
CR model	−19.69	86.87	−39.00	130.61	−82.26	203.61
B-CR model, $r_{\min} = 0$	−21.32	86.54	−42.01	130.03	−86.32	202.61
B-CR model, $r_{\min}$ free	−21.78	86.61	−42.41	130.04	−86.47	202.08
Five-year yield						
Random walk	−17.02	74.15	−29.19	98.38	−58.79	137.49
CR model	−24.38	73.83	−40.66	98.68	−76.62	140.18
B-CR model, $r_{\min} = 0$	−25.09	74.09	−41.93	99.08	−78.38	140.78
B-CR model, $r_{\min}$ free	−24.80	74.10	−41.48	98.98	−77.87	140.79
Ten-year yield						
Random walk	−12.76	59.13	−20.87	72.80	−42.42	84.95
CR model	−7.21	56.33	−18.34	69.85	−44.06	85.19
B-CR model, $r_{\min} = 0$	−7.81	56.52	−19.27	70.32	−45.40	86.24
B-CR model, $r_{\min}$ free	−7.68	56.52	−19.17	70.33	−45.52	86.34

Notes: Summary statistics of the forecast errors—mean and root-mean-square errors (RMSEs) — of the three-month, two-year, five-year, and 10-year U.S. Treasury yields six months, one year, and two years ahead. The forecasts are weekly during the normal period from January 6, 1995, to December 12, 2008, a total of 728 forecasts for all three forecast horizons. All measurements are expressed in basis points.

yields are near the ZLB implies notably poorer yield forecast performance at longer forecast horizons, except for the longest yield maturity.

4.4. Decomposing 10-Year Yields

One important use for affine DTSMs has been to separate longer-term yields into a short-rate expectations component and a term premium.

Table 6. Summary Statistics for Forecast Errors of U.S. Treasury Yields in the ZLB Period.

	Six-Month Forecast		One-Year Forecast		Two-Year Forecast	
	Mean	RMSE	Mean	RMSE	Mean	RMSE
Three-month yield						
Random walk	−1.34	6.45	−2.15	7.17	−4.63	7.36
CR model	−6.87	26.29	−19.02	42.16	−64.52	79.07
B-CR model, $r_{\min} = 0$	−16.98	19.68	−33.42	35.80	−74.04	78.55
B-CR model, $r_{\min}$ free	−21.04	23.78	−38.69	41.38	−85.16	89.05
Two-year yield						
Random walk	−3.45	23.04	−9.84	26.13	−22.60	41.34
CR model	−18.08	31.03	−47.88	54.65	−113.68	119.87
B-CR model, $r_{\min} = 0$	−22.12	35.08	−49.83	60.62	−110.02	123.05
B-CR model, $r_{\min}$ free	−25.01	37.33	−56.35	66.12	−122.44	133.21
Five-year yield						
Random walk	−2.98	55.31	−11.73	68.57	−38.34	103.11
CR model	−28.11	60.93	−62.11	90.52	−134.98	165.32
B-CR model, $r_{\min} = 0$	−27.41	63.31	−60.34	94.92	−132.49	169.35
B-CR model, $r_{\min}$ free	−31.41	65.58	−67.18	99.19	−142.71	175.32
Ten-year yield						
Random walk	−8.36	67.36	−19.44	88.00	−55.95	126.57
CR model	−21.59	74.46	−48.09	103.45	−115.63	167.99
B-CR model, $r_{\min} = 0$	−25.63	74.87	−52.74	106.28	−120.74	171.23
B-CR model, $r_{\min}$ free	−25.97	73.41	−55.67	105.40	−125.41	171.62

Notes: Summary statistics of the forecast errors—mean and root-mean-square errors (RMSEs)—of the three-month, two-year, five-year, and 10-year U.S. Treasury yields six months, one year, and two years ahead. The forecasts are weekly during the zero lower bound period that starts on December 19, 2008, and runs until May 2, 2014, for the six-month forecasts (281 forecasts), until November 1, 2013, for the one-year forecasts (255 forecasts), and until November 2, 2012, for the two-year forecasts (203 forecasts). All measurements are expressed in basis points.

Here, we document the different decompositions of the 10-year Treasury yield implied by the CR and B-CR models. To do so, we calculate, for each end date during our rolling re-estimation period, the average expected path for the overnight rate, $(1/\tau)\int_t^{t+\tau} E_t^P[r_s]\mathrm{d}s$, as well as the associated term premium — assuming the two components sum to the fitted bond yield, $\hat{y}_t(\tau)$.[28]

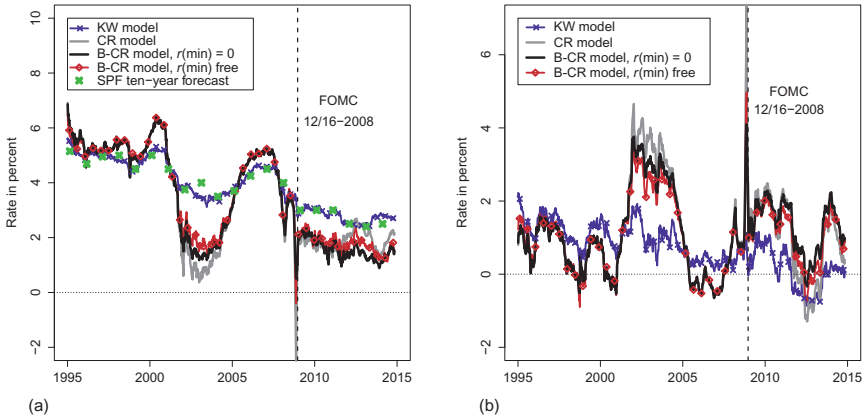

Fig. 14. Ten-Year Expected Short Rate and Term Premium. *Notes:* Panel (a) provides real-time estimates of the average policy rate expected over the next 10 years from the CR and B-CR models, where the latter is estimated with $r_{\min}$ both restricted to zero and left free. Also shown are the corresponding estimates form the KW model and the annual forecasts of the average three-month Treasury bill rate over the next 10 years from the SPF. Panel (b) shows the corresponding real-time

Fig. 14 shows the real-time decomposition of the 10-year Treasury yield into a policy expectations component and a term premium component according to the CR and B-CR models, again with a comparison to the corresponding estimates from the KW model. Studying the time-series patterns in greater detail, we first note the similar decompositions from the CR and B-CR model until December 2008 – with the notable exception of the 2002–2004 period when yields were low the last time. Second, we see some smaller discrepancies across these two model decompositions in the period between December 2008 and August 2011. Finally, we point out the sustained difference in the extracted policy expectations and term premiums in the period from August 2011 through 2012 when yields of all maturities reached historical low levels.

Also shown in Fig. 14(a) are long-term forecasts of average short rates from the Survey of Professional Forecasters (SPF) – specifically, the median of respondents' expectations for the average three-month Treasury bill rate over the next 10 years.[29] First, we note that the short-rate expectations from the survey are less variable and higher on average than those

produced by the CR and B-CR models. Second, it is clear that the KW model's short-rate expectations track the survey expectations quite closely. This is not surprising since survey data, admittedly from a different source (the Blue Chip Financial Forecasts), are used as an input in its empirical implementation.

Finally, we note that Fig. 14 suggests that, at least through late 2011, the ZLB did not greatly affect the term premium decomposition of the CR model. To provide a concrete example of this, we repeat the analysis in CR of the Treasury yield response to eight key announcements by the Fed regarding its first large-scale asset purchase (LSAP) program. Table 7 shows the CR and B-CR model decompositions of the 10-year U.S. Treasury yield on these eight dates and the total changes.[30] The yield decompositions on these dates are quite similar for both of these models, though the B-CR model ascribes a bit more of the changes in yields to a signaling channel effect adjusting short-rate expectations. Hence, the conclusions of CR about the effects of the Fed's first LSAP program on U.S. Treasury yields are robust to the use of a shadow-rate model.

4.5. Assessing Recent Shifts in Near-Term Monetary Policy Expectations

In this section, we attempt to assess the extent to which the models are able to capture recent shifts in near-term monetary policy expectations.

To do so, we compare the variation in the models' one- and two-year short-rate forecasts since 2007 to the rates on one- and two-year federal funds futures contracts as shown in Fig. 15.[31] We note that the existence of time-varying risk premiums even in very short-term federal funds futures contracts is well documented (see Piazzesi & Swanson, 2008). However, the risk premiums in such short-term contracts are small relative to the sizeable variation over time observed in Fig. 15. As a consequence, we interpret the bulk of the variation from 2007 to 2009 as reflecting declines in short-rate expectations.

Furthermore, since August 2011, most evidence – including the low yield volatility shown in Fig. 12 – suggests that risk premiums have been significantly depressed, likely to a point that a zero-risk-premium assumption for the futures contracts discussed here is a satisfactory approximation. Combined these observations suggest that it is defensible for most of the shown eight-year period to map the models' short-rate projections to the rates on the federal funds futures contracts *without* adjusting for their risk premiums.

Table 7. Decomposition of Responses of 10-Year U.S. Treasury Yield.

Announcement Date	Model	Decomposition from Models			10-Year Treasury Yield
		Avg. target rate next 10 years	10-year term premium	Residual	
Nov. 25, 2008	CR	−20	0	−2	−21
	B-CR	−10	−10	0	
Dec. 1, 2008	CR	−10	−10	−2	−22
	B-CR	−21	2	−3	
Dec. 16, 2008	CR	−7	−7	−3	−17
	B-CR	−17	3	−3	
Jan. 28, 2009	CR	6	1	5	12
	B-CR	9	−2	5	
Mar. 18, 2009	CR	−14	−23	−15	−52
	B-CR	−17	−20	−14	
Aug. 12, 2009	CR	−1	1	6	6
	B-CR	−4	4	6	
Sep. 23, 2009	CR	−5	2	1	−2
	B-CR	−3	1	1	
Nov. 4, 2009	CR	−1	5	3	7
	B-CR	−1	5	3	
Total net change	CR	−53	−29	−7	−89
	B-CR	−65	−17	−7	

Notes: The decomposition of responses of the 10-year U.S. Treasury yield on eight LSAP announcement dates into changes in (i) the average expected target rate over the next 10 years, (ii) the 10-year term premium, and (iii) the unexplained residual based on the CR and B-CR models, where the latter is estimated with $r_{\min}$ restricted to zero. All changes are measured in basis points.

At the one- and two-year forecast horizons, the correlations between the short-rate forecasts from the models and the federal funds futures rates are all quite high. The KW model has the highest correlations, 97.7 and 95.1 percent, at the one- and two-year horizon, respectively, followed by the B-CR model with $r_{\min}$ restricted to zero, which has correlations of 97.0 and 90.5 percent at the one- and two-year horizon, respectively.[32] The CR model has the lowest correlations, 88.3 and 68.7 percent. If, instead, a distance metric is used, the performance across models is more varied. Table 8 reports the mean deviations and the root-mean-square deviations (RMSDs) from all four models relative to the rates of the federal funds futures contracts. For the CR model, the distance to the futures rates measured by RMSDs is 79.61 and 124.77 basis points at the one- and two-year horizon, respectively. The KW model also shows a

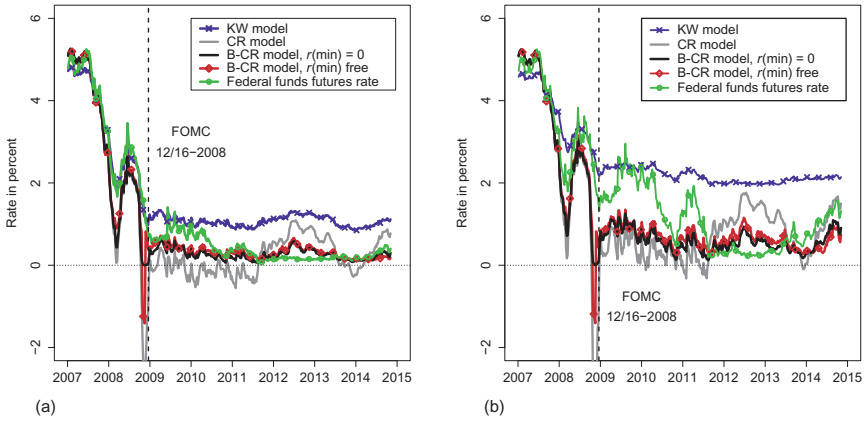

Fig. 15. Comparison of Short-Rate Projections. *Notes:* Panel (a) illustrates the one-year short-rate projections from the CR and B-CR models, where the latter is estimated with $r_{\min}$ both restricted to zero and left free. Also shown are the corresponding estimates form the KW model and the rates on one-year federal funds futures. Panel (b) shows the corresponding results for a two-year projection period with a comparison to the rates on two-year federal funds futures. The data are weekly covering the period from January 5, 2007, to October 31, 2014.

poor match with RMSDs of 66.38 and 110.12 basis points at the one- and two-year horizons, while the two shadow-rate models provide a much closer fit to the futures rates during the period under analysis. Thus, both measured by correlations and by a distance metric, the B-CR model's short-rate projections appear to be better aligned with the information reflected in rates on federal funds futures than the projections generated by the standard CR model, and this conclusion is not sensitive to the choice of lower bound.

5. CONCLUSION

In this paper, we study the performance of a standard Gaussian DTSM of U.S. Treasury yields and its equivalent shadow-rate version. This provides us with a clean read on the merits of casting a standard model as a shadow-rate model to respect the ZLB of nominal yields.

Table 8. Summary Statistics of Differences relative to Federal Funds Futures Rates.

Model	One-Year Contract		Two-Year Contract	
	Mean	RMSD	Mean	RMSD
KW model	49.54	66.38	86.84	110.12
CR model	−28.73	79.61	−46.99	124.77
B-CR, $r_{\min} = 0$	−19.26	40.92	−47.11	76.17
B-CR, $r_{\min}$ free	−14.56	41.68	−39.83	75.37

Notes: The mean deviations and the root-mean-square deviations (RMSDs) between the short-rate expectations from four term structure models, on one side, and federal funds futures rates, on the other, are reported for two contract horizons. In each case, the summary statistics are calculated for the periods from January 5, 2007, to October 31, 2014. All numbers are measured in basis points.

We find that the standard model performed well until the end of 2008 but underperformed since then. In the current near-ZLB yield environment, we find that the shadow-rate model provides superior in-sample fit, matches the compression in yield volatility unlike the standard model, and delivers better real-time short-rate forecasts. Thus, while one could expect the regular model to get back on track as soon as short- and medium-term yields rise from their current low levels, our findings suggest that, in the meantime, shadow-rate models offer a tractable way of mitigating the problems related to the ZLB constraint on nominal yields. For a practical application of the shadow-rate model that takes advantage of its accurate forecasts near the ZLB, see Christensen, Lopez, and Rudebusch (2015).

However, allowing for a nonzero lower bound for the short rate determined by quasi maximum likelihood provides at best only modest gains in model performance at the cost of unrealistically large estimates of the lower bound before the financial crisis. Thus, we consider this added complexity unnecessary and strongly recommend setting the lower bound at zero for U.S. Treasury yields. Of course, as the recent experience of negative sovereign yields in Europe demonstrates, the lower bound is not in general always equal to zero. How to determine this possibly time-varying constraint on nominal yields remains an important topic for further research. In addition, differences between yield curve dynamics in normal and ZLB periods could reflect deeper nonlinearities in the factor structure, or maybe even a regime switch in the factor dynamics as argued in Christensen (2015), that are beyond the static affine dynamic structure assumed in this paper. This also remains an open question for future research.

NOTES

1. Diebold and Rudebusch (2013) and Krippner (2015) provide comprehensive discussions on the AFNS model with and without the ZLB.

2. Following Kim and Singleton (2012), the prefix "B-" refers to a shadow-rate model in the spirit of Black (1995).

3. Kim and Priebsch (2013) estimate the lower bound in their shadow-rate model, but do not make a comprehensive assessment of the implications of doing so.

4. Bauer and Rudebusch (2014) show that estimated shadow-rate paths are very sensitive to the choice of lower bound, which is consistent with our results.

5. Bauer and Rudebusch (2014) is a study that uses this approach.

6. Note that a Jensen's inequality term has been left out for the rollover strategy in this definition.

7. Difficulties in estimating Gaussian term structure models are discussed in Christensen et al. (2011), who propose using a Nelson−Siegel structure to avoid them. See Joslin, Singleton, and Zhu (2011), Hamilton and Wu (2012), and Andreasen and Christensen (2015) for alternative approaches to facilitate estimation of Gaussian DTSMs.

8. Two details regarding this specification are discussed in Christensen et al. (2011). First, with a unit root in the level factor under the Q-measure, the model is not arbitrage free with an unbounded horizon; therefore, as is often done in theoretical discussions, we impose an arbitrary maximum horizon. Second, we identify this class of models by normalizing the $\boldsymbol{\theta}^Q$ means under the Q-measure to zero without loss of generality.

9. As noted in Christensen et al. (2011), the unconstrained AFNS model has a sign restriction and three parameters less than the standard canonical three-factor Gaussian DTSM.

10. Due to the unit-root property of the first factor, we can arbitrarily fix its mean at $\theta_1^P = 0$.

11. The yield data include three- and six-month Treasury bill yields from the H.15 series from the Federal Reserve Board as well as off-the-run Treasury zero-coupon yields for the remaining maturities from the Gürkaynak, Sack, and Wright (2007) database, which is available at http://www.federalreserve.gov/pubs/feds/2006/200628/200628abs.html.

12. That is, a test of the joint hypothesis $\kappa_{12}^P = \kappa_{13}^P = \kappa_{31}^P = \kappa_{32}^P = 0$ using a standard likelihood ratio test. Note also that this test is done *before* imposing the unit-root property.

13. For example, Kim and Singleton (2012) and Bomfim (2003) use finite-difference methods to calculate bond prices, while Ichiue and Ueno (2007) employ interest rate lattices.

14. Wu and Xia (2014) derive a discrete-time version of the Krippner framework and implement a three-factor specification using U.S. Treasury data. In related research, Priebsch (2013) derives a second-order approximation to the Black (1995) shadow-rate model and estimates a three-factor version thereof, but it requires the calculation of a double integral in contrast to the single integral needed to fit the yield curve in the Krippner framework. Krippner (2015) provides a definitive treatment.

15. In particular, there is no explicit partial differential equation (PDE) that bond prices must satisfy, including boundary conditions, for the absence of arbitrage as in Kim and Singleton (2012).

16. For details of the derivations, see Christensen and Rudebusch (2015).

17. Due to the nonlinear measurement equation for the yields in the shadow-rate AFNS model, estimation is based on the standard extended Kalman filter as described in Christensen and Rudebusch (2015) and referred to as quasi maximum likelihood. We also estimated unrestricted and independent factor shadow-rate AFNS models and obtained similar results to those reported below.

18. That is, a test of the joint hypothesis $\kappa_{12}^P = \kappa_{13}^P = \kappa_{31}^P = \kappa_{32}^P = 0$ using a quasi likelihood ratio test. As with the CR model, this test is performed *before* imposing the unit-root property.

19. Consistent with our series for the 2003-period, Bomfim (2003) in his calibration of a two-factor shadow-rate model to U.S. interest rate swap data reports a probability of hitting the zero-boundary within the next two years equaling 3.6 percent as of January 2003. Thus, it appears that bond investors did not perceive the risk of reaching the ZLB during the 2003−2004 period of low interest rates to be material.

20. Note that for $r_{\min} \to -\infty$ it holds that $f_t(\tau) \to f_t(\tau)$ for any t and all $\tau > 0$.

21. For Japan, Ichiue and Ueno (2013) impose a lower bound of nine basis points from January 2009 to December 2012 and reduce it to five basis points thereafter. For the United States, they use a lower bound of 14 basis points starting in November 2009. Finally, for the United Kingdom, they assume the standard ZLB for the short rate.

22. Christensen and Rudebusch (2015) report support for zero as a lower bound in Japanese government bond yields.

23. The conditional covariance matrix is calculated using the analytical solutions provided in Fisher and Gilles (1996).

24. Note that other measures of realized volatility have been used in the literature, such as the realized mean absolute deviation measure as well as fitted GARCH estimates. Collin-Dufresne et al. (2009) also use option-implied volatility as a measure of realized volatility.

25. In their analysis of Japanese government bond yields, Kim and Singleton (2012) also report a close match to yield volatilities for their Gaussian shadow-rate model.

26. Appendix B contains the formulas used to calculate short-rate projections.

27. The KW model is estimated using one-, two-, four-, seven-, and 10-year off-the-run Treasury zero-coupon yields from the Gürkaynak et al. (2007) database, as well as three- and six-month Treasury bill yields. To facilitate empirical implementation, model estimation includes monthly data on the six- and 12-month-ahead forecasts of the three-month T-bill yield from Blue Chip Financial Forecasts and semiannual data on the average expected three-month T-bill yield six to 11 years hence from the same source. For updated data provided by the staff of the Federal Reserve Board, see http://www.federalreserve.gov/econresdata/researchdata/feds200533.html.

28. The details of these calculations for both the CR and B-CR model are provided in appendices B and C.

29. The SPF is normally performed quarterly and only include questions about shorter-term expectations, but once a year respondents are asked about their long-term expectations. It is the median of the responses to this question that is shown in the figure. The data are available at http://www.philadelphiafed.org/research-and-data/real-time-center/survey-of-professional-forecasters/.

30. Due to the computational burden of estimating the B-CR model on this daily yield sample, we only perform this exercise for the B-CR model with $r_{\min}$ restricted to zero.

31. The futures data are from Bloomberg. The one-year futures rate is the weighted average of the rates on the 12- and 13-month federal funds futures contracts, while the two-year futures rate is the rate on the 24-month federal funds futures contract through 2010, and the weighted average of the rates on the 24- and 25-month contracts since then. The absence of data on the 24-month contracts prior to 2007 determines the start date for the analysis.

32. The B-CR model without restrictions on $r_{\min}$ has one- and two-year correlations of 96.4 and 89.0 percent, respectively.

33. Of course, away from the ZLB, with a negligible call option, the model will match the standard arbitrage-free term structure representation.

34. We calculate the conditional covariance matrix using the analytical solutions provided in Fisher and Gilles (1996).

ACKNOWLEDGMENTS

We thank two anonymous referees, Martin Møller Andreasen as well as conference participants at the FRBSF Workshop on "Term Structure Modeling at the Zero Lower Bound," the 20th International Conference on Computing in Economics and Finance, the First Annual Conference of the International Association for Applied Econometrics, and the Banque de France Workshop on "Term Structure Modeling and the Zero Lower Bound" – especially Don Kim and Jean-Paul Renne – for helpful comments. The views in this paper are solely the responsibility of the authors and should not be interpreted as reflecting the views of the Federal Reserve Bank of San Francisco or the Board of Governors of the Federal Reserve System. We thank Lauren Ford and Simon Riddell for excellent research assistance.

REFERENCES

Andersen, T. G., & Benzoni, L. (2010). Do bonds span volatility risk in the U.S. treasury market? A specification test for affine term structure models. *Journal of Finance*, *65*(2), 603–653.

Andreasen, M. M., & Christensen, B. J. (2015). The SR approach: A new estimation procedure for non-linear and non-gaussian dynamic term structure models. *Journal of Econometrics*, *184*(2), 420−451.

Andreasen, M. M., & Meldrum, A. (2014). *Dynamic term structure models: The best way to enforce the zero lower bound*. CREATES Research Paper No. 2014-47, Aarhus University, Department of Economics and Business.

Bauer, M. D., & Rudebusch, G. D. (2014). *Monetary policy expectations at the zero lower bound*. Federal Reserve Bank of San Francisco, Working Paper No. 2013-18.

Bauer, M. D., Rudebusch, G. D., & Wu, J. C. (2012). Correcting estimation bias in dynamic term structure models. *Journal of Business Economics and Statistics*, *30*(3), 454−467.

Black, F. (1995). Interest rates as options. *Journal of Finance*, *50*(7), 1371−1376.

Bomfim, A. N. (2003). Interest rates as options: 'Assessing the markets' view of the liquidity trap, Working Paper No. 2003-45. *Finance and Economics Discussion Series*, Federal Reserve Board, Washington, DC.

Christensen, J. H. E. (2015). *A regime-switching model of the yield curve at the zero bound*. Working Paper No. 2013-34, Federal Reserve Bank of San Francisco.

Christensen, J. H. E., Diebold, F. X., & Rudebusch, G. D. (2011). The affine arbitrage-free class of Nelson-Siegel term structure models. *Journal of Econometrics*, *164*(1), 4−20.

Christensen, J. H. E., Lopez, J. A., & Rudebusch, G D. (2015). A probability-based stress test of Federal Reserve assets and income. *Journal of Monetary Economics, first published online*, *8*, doi: 10.1016/j.jmoneco.2015.03.007.

Christensen, J. H. E., & Rudebusch, G. D. (2012). The response of interest rates to U.S. and U.K. quantitative easing. *Economic Journal*, *122*, 385−414.

Christensen, J. H. E., & Rudebusch, G. D. (2015). Estimating shadow-rate term structure models with near-zero yields. *Journal of Financial Econometrics*, *13*(2), 226−259.

Collin-Dufresne, P., Goldstein, R S., & Jones, C S. (2009). Can interest rate volatility be extracted from the cross-section of bond yields? *Journal of Financial Economics*, *94*(1), 47−66.

Diebold, F. X., & Rudebusch, G. D. (2013). *Yield curve modeling and forecasting: The dynamic Nelson-Siegel approach*. Princeton, NJ: Princeton University Press.

Duffee, G. R. (2002). Term premia and interest rate forecasts in affine models. *Journal of Finance*, *57*(1), 405−443.

Duffie, D., & Kan, R. (1996). A yield-factor model of interest rates. *Mathematical Finance*, *6*(4), 379−406.

Filipović, D., Larsson, M., & Trolle, A. (2014). Linear-rational term structure models. *Manuscript Swiss Finance Institute*.

Fisher, M., & Gilles, C. (1996). Term premia in exponential-affine models of the term structure. *Manuscript Board of Governors of the Federal Reserve System*.

Gürkaynak, R. S., Sack, B., & Wright, J. H. (2007). The U.S. treasury yield curve: 1961 to the present. *Journal of Monetary Economics*, *54*(8), 2291−2304.

Hamilton, J. D., & Wu, J. C. (2012). Identification and estimation of Gaussian affine term structure models. *Journal of Econometrics*, *168*(2), 315−331.

Ichiue, H., & Ueno, Y. (2007). *Equilibrium interest rates and the yield curve in a low interest rate environment*, Working Paper No. 2007-E-18, Bank of Japan.

Ichiue, H., & Ueno, Y. (2013). *Estimating term premia at the zero bound: An analysis of Japanese, US, and UK Yields*, Working Paper No. 2013-E-8, Bank of Japan.

Jacobs, K., & Karoui, L. (2009). Conditional volatility in affine term structure models: Evidence from treasury and swap markets. *Journal of Financial Economics*, *91*(3), 288−318.

Joslin, S., Singleton, K J., & Zhu, H. (2011). A new perspective on Gaussian dynamic term structure models. *Review of Financial Studies*, *24*(3), 926−970.

Kim, D. H., & Priebsch, M. (2013). *Estimation of multi-factor shadow-rate term structure models*, Washington, DC: Federal Reserve Board.

Kim, D. H., & Singleton, K. J. (2012). Term structure models and the zero bound: An empirical investigation of Japanese yields. *Journal of Econometrics*, *170*(1), 32−49.

Kim, D. H., & Wright, J H. (2005). *An arbitrage-free three-factor term structure model and the recent behavior of long-term yields and distant-horizon forward rates*. Working Finance and Economics Discussion Series 2055-33, Board of Governors of the Federal Reserve System.

Krippner, L. (2013). *A tractable framework for zero lower bound Gaussian term structure models*. Discussion Paper No. 2013-02, Reserve Bank of New Zealand.

Krippner, L. (2015). *Term structure modeling at the zero lower bound: A practitioner's guide*, New York, NY: Palgrave-Macmillan.

Monfort, A., Pegoraro, F., Renne, J-P., & Roussellet, G. (2014). Staying at zero with affine processes: A new dynamic term structure model. *Manuscript Banque de France*.

Nelson, C. R., & Siegel, A. F. (1987). Parsimonious modeling of yield curves. *Journal of Business*, *60*(4), 473−489.

Piazzesi, M., & Swanson, E. T. (2008). Futures Prices as Risk-Adjusted Forecasts of Monetary Policy. *Journal of Monetary Economics*, *55*(4), 677−691.

Priebsch, M. (2013). *Computing arbitrage-free yields in multi-factor gaussian shadow-rate term structure models*. Finance and Economics Discussion Series Working Paper No. 2013-63, Board of Governors of the Federal Reserve System.

Wu, C ., & Xia, F D. (2014). Measuring the macroeconomic impact of monetary policy at the zero lower bound. *Manuscript, University of California at San Diego*.

APPENDIX A: HOW GOOD IS THE OPTION-BASED APPROXIMATION?

As noted in Section 3.1, Krippner (2013) does not provide a formal derivation of arbitrage-free pricing relationships for the option-based approach. Therefore, in this appendix, we analyze how closely the option-based bond pricing from the estimated B-CR model matches an arbitrage-free bond pricing that is obtained from the same model using Black's (1995) approach based on Monte Carlo simulations. The simulation-based shadow yield curve is obtained from 50,000 10-year long factor paths generated using the estimated Q-dynamics of the state variables in the B-CR model, which, ignoring the nonnegativity equation (5), are used to construct 50,000 paths for the shadow short rate. These are converted into a corresponding number of shadow discount bond paths and averaged for each maturity before the resulting shadow discount bond prices are converted into yields. The simulation-based yield curve is obtained from the same underlying 50,000 Monte Carlo factor paths, but at each point in time in the simulation, the resulting short rate is constrained by the nonnegativity equation (5) as in Black (1995). The shadow-rate curve from the B-CR model can also be calculated analytically via the usual affine pricing relationships, which ignore the ZLB. Thus, any difference between these two curves is simply numerical error that reflects the finite number of simulations.

To document that the close match between the option-based and the simulation-based yield curves is not limited to any specific date where the ZLB of nominal yields is likely to have mattered, we undertake this simulation exercise for the last observation date in each year since 2006.[33] Table A1 reports the resulting shadow yield curve differences and yield curve differences for various maturities on these nine dates. Note that the errors for the shadow yield curves solely reflect simulation error as the model-implied shadow yield curve is identical to the analytical arbitrage-free curve that would prevail without currency in circulation. These simulation errors in Table A1 are typically very small in absolute value, and they increase only slowly with maturity. Their average absolute value − shown in the bottom row − is less than one basis point even at a 10-year maturity. This implies that using simulations with a large number of draws ($N =$ 50,000) arguably delivers enough accuracy for the type of inference we want to make here.

Given this calibration of the size of the numerical errors involved in the simulation, we can now assess the more interesting size of the approximation

Table A1. Approximation Errors in Yields for Shadow-Rate Model.

Dates		Maturity in Months				
		12	36	60	84	120
12/29/06	Shadow yields	0.30	−0.73	−1.22	−1.08	−1.10
	Yields	0.33	−0.71	−1.13	−0.87	−0.52
12/28/07	Shadow yields	0.17	0.02	0.65	0.86	0.79
	Yields	0.22	0.16	0.85	1.18	1.28
12/26/08	Shadow yields	−0.01	0.51	0.56	0.45	0.28
	Yields	0.09	0.76	1.51	1.93	2.26
12/31/09	Shadow yields	0.10	0.63	1.18	1.28	1.08
	Yields	0.04	0.74	1.46	1.69	1.68
12/31/10	Shadow yields	−0.21	−0.11	−0.10	−0.16	0.00
	Yields	−0.10	0.45	0.86	1.03	1.39
12/30/11	Shadow yields	0.19	0.88	1.11	1.51	1.92
	Yields	−0.02	0.68	1.80	3.11	4.56
12/28/12	Shadow yields	0.11	−0.35	−0.48	−0.26	−0.09
	Yields	0.13	0.35	1.28	2.48	3.79
12/27/13	Shadow yields	−0.17	−0.17	0.25	0.25	0.14
	Yields	0.06	0.70	1.60	2.00	2.20
10/31/14	Shadow yields	0.30	0.22	−0.10	−0.25	−0.13
	Yields	0.21	0.66	0.84	1.13	1.92
Average abs. diff	Shadow yields	0.16	0.46	0.76	0.80	0.75
	Yields	0.13	0.55	1.27	1.76	2.21

Notes: At each date, the table reports differences between the analytical shadow yield curve obtained from the option-based estimates of the B-CR model and the shadow yield curve obtained from 50,000 simulations of the estimated factor dynamics under the Q-measure in that model. The table also reports for each date the corresponding differences between the fitted yield curve obtained from the B-CR model and the yield curve obtained via simulation of the estimated B-CR model with imposition of the ZLB. The bottom two rows give averages of the absolute differences across the 9 dates. All numbers are measured in basis points.

error in the option-based approach to valuing yields in the presence of the ZLB. In Table A1, the errors of the fitted B-CR model yield curves relative to the simulated results are only slightly larger than those reported for the shadow yield curve. In particular, for maturities up to five years, the errors tend to be less than 1 basis point, so the option-based approximation error adds very little if anything to the numerical simulation error. At the 10-year maturity, the approximation errors are understandably larger, but even the largest errors at the 10-year maturity do not exceed 4 basis points in absolute value and the average absolute value is less than 2 basis points. Overall, the option-based approximation errors in our three-factor setting appear

relatively small. Indeed, they are smaller than the fitted errors to be reported in Table 3. That is, for the B-CR model analyzed here, the gain from using a numerical estimation approach instead of the option-based approximation would in all likelihood be negligible.

APPENDIX B: FORMULA FOR POLICY EXPECTATIONS IN AFNS AND B-AFNS MODELS

In this appendix, we detail how conditional expectations for future policy rates are calculated within AFNS and B-AFNS models.

In affine models, in general, the conditional expected value of the state variables is calculated as

$$E_t^P[X_{t+\tau}] = \left(I - \exp\left(-K^P\tau\right)\right)\theta^P + \exp\left(-K^P\tau\right)X_t$$

In AFNS models, the instantaneous short rate is defined as

$$r_t = L_t + S_t$$

Thus, the conditional expectation of the short rate is

$$E_t^P[r_{t+\tau}] = E_t^P[L_{t+\tau} + S_{t+\tau}] = \begin{pmatrix} 1 & 1 & 0 \end{pmatrix} E_t^P[X_{t+\tau}]$$

In B-AFNS models, the instantaneous shadow rate is defined as

$$s_t = L_t + S_t$$

In turn, the conditional expectation of the shadow-rate process is

$$E_t^P[s_{t+\tau}] = E_t^P[L_{t+\tau} + S_{t+\tau}] = \begin{pmatrix} 1 & 1 & 0 \end{pmatrix} E_t^P[X_{t+\tau}]$$

Now, the conditional covariance matrix of the state variables is given by[34]

$$V_t^P[X_{t+\tau}] = \int_0^\tau \mathrm{e}^{-K^P s}\Sigma\Sigma'\mathrm{e}^{-(K^P)'s}\mathrm{d}s$$

Hence, the conditional covariance of the shadow-rate process is

$$V_t^P[s_{t+\tau}] = \begin{pmatrix} 1 & 1 & 0 \end{pmatrix} V_t^P[X_{t+\tau}] \begin{pmatrix} 1 \\ 1 \\ 0 \end{pmatrix}$$

Finally, following equation (65) in Kim and Singleton (2012), the conditional expectation of the short rate in the B-AFNS models,

$$r_t = \max(r_{\min}, s_t)$$

is given by

$$\begin{aligned} E^P[r_{t+\tau}] &= \int_{-\infty}^{\infty} r_{t+\tau} f(r_{t+\tau}|X_t) \mathrm{d}r_{t+\tau} = r_{\min} + \int_{r_{\min}}^{\infty} (s_{t+\tau} - r_{\min}) f(s_{t+\tau}|X_t) \mathrm{d}s_{t+\tau} \\ &= r_{\min} + \left(E_t^P[s_{t+\tau}] - r_{\min}\right) N\left(\frac{\left(E_t^P[s_{t+\tau}] - r_{\min}\right)}{\sqrt{V_t^P[s_{t+\tau}]}}\right) \\ &\quad + \frac{1}{\sqrt{2\pi}} \sqrt{V_t^P[s_{t+\tau}]} \quad \exp\left(-\frac{1}{2} \frac{\left(E_t^P[s_{t+\tau}] - r_{\min}\right)^2}{V_t^P[s_{t+\tau}]}\right) \end{aligned}$$

APPENDIX C: ANALYTICAL FORMULAS FOR AVERAGES OF POLICY EXPECTATIONS AND FOR TERM PREMIUMS IN THE CR MODEL

In this appendix, we derive the analytical formulas for averages of policy expectations and for term premiums within the CR model.

For a start, the term premium is defined as

$$TP_t(\tau) = y_t(\tau) - \frac{1}{\tau} \int_t^{t+\tau} E_t^P[r_s] \mathrm{d}s$$

In the CR model, as in any AFNS model, the instantaneous short rate is defined as

$$r_t = L_t + S_t$$

while the specification of the P-dynamics is given by

$$\begin{pmatrix} \mathrm{d}L_t \\ \mathrm{d}S_t \\ \mathrm{d}C_t \end{pmatrix} = \begin{pmatrix} 10^{-7} & 0 & 0 \\ \kappa_{21}^P & \kappa_{22}^P & \kappa_{23}^P \\ 0 & 0 & \kappa_{33}^P \end{pmatrix} \left[\begin{pmatrix} 0 \\ \theta_2^P \\ \theta_3^P \end{pmatrix} - \begin{pmatrix} L_t \\ S_t \\ C_t \end{pmatrix} \right] \mathrm{d}t + \begin{pmatrix} \sigma_{11} & 0 & 0 \\ 0 & \sigma_{22} & 0 \\ 0 & 0 & \sigma_{33} \end{pmatrix} \begin{pmatrix} \mathrm{d}W_t^{L,P} \\ \mathrm{d}W_t^{S,P} \\ \mathrm{d}W_t^{C,P} \end{pmatrix}$$

Thus, the mean-reversion matrix is given by

$$K^P = \begin{pmatrix} 10^{-7} & 0 & 0 \\ \kappa_{21}^P & \kappa_{22}^P & \kappa_{23}^P \\ 0 & 0 & \kappa_{33}^P \end{pmatrix}$$

Its matrix exponential can be calculated analytically:

$$\exp\left(-K^P\tau\right) = \begin{pmatrix} 1 & 0 & 0 \\ -\kappa_{21}^P \dfrac{1-\mathrm{e}^{-\kappa_{22}^P\tau}}{\kappa_{22}^P} & \mathrm{e}^{-\kappa_{22}^P\tau} & -\kappa_{23}^P \dfrac{\mathrm{e}^{-\kappa_{33}^P\tau}-\mathrm{e}^{-\kappa_{22}^P\tau}}{\kappa_{22}^P-\kappa_{33}^P} \\ 0 & 0 & \mathrm{e}^{-\kappa_{33}^P\tau} \end{pmatrix}$$

Now, the conditional mean of the state variables is

$$\begin{aligned} E_t^P[X_{t+\tau}] &= \theta^P + \begin{pmatrix} 1 & 0 & 0 \\ -\kappa_{21}^P \dfrac{1-\mathrm{e}^{-\kappa_{22}^P\tau}}{\kappa_{22}^P} & \mathrm{e}^{-\kappa_{22}^P\tau} & -\kappa_{23}^P \dfrac{\mathrm{e}^{-\kappa_{33}^P\tau}-\mathrm{e}^{-\kappa_{22}^P\tau}}{\kappa_{22}^P-\kappa_{33}^P} \\ 0 & 0 & \mathrm{e}^{-\kappa_{33}^P\tau} \end{pmatrix} \begin{pmatrix} L_t \\ S_t-\theta_2^P \\ C_t-\theta_3^P \end{pmatrix} \\ &= \begin{pmatrix} L_t \\ \theta_2^P - \kappa_{21}^P \dfrac{1-\mathrm{e}^{-\kappa_{22}^P\tau}}{\kappa_{22}^P} L_t + \mathrm{e}^{-\kappa_{22}^P\tau}\left(S_t-\theta_2^P\right) - \kappa_{23}^P \dfrac{\mathrm{e}^{-\kappa_{33}^P\tau}-\mathrm{e}^{-\kappa_{22}^P\tau}}{\kappa_{22}^P-\kappa_{33}^P}\left(C_t-\theta_3^P\right) \\ \theta_3^P + \mathrm{e}^{-\kappa_{33}^P\tau}\left(C_t-\theta_3^P\right) \end{pmatrix} \end{aligned}$$

In order to get back to the term premium formula, we note that the conditional expectation of the instantaneous short-rate process is given by

$$
\begin{aligned}
E_t^P[r_s] &= E_t^P[L_s + S_s] \\
&= \left(1 - \kappa_{21}^P \frac{1 - \mathrm{e}^{-\kappa_{22}^P(s-t)}}{\kappa_{22}^P}\right) L_t + \theta_2^P + \mathrm{e}^{-\kappa_{22}^P(s-t)}\left(S_t - \theta_2^P\right) \\
&\quad - \kappa_{23}^P \frac{\mathrm{e}^{-\kappa_{33}^P(s-t)} - \mathrm{e}^{-\kappa_{22}^P(s-t)}}{\kappa_{22}^P - \kappa_{33}^P}\left(C_t - \theta_3^P\right)
\end{aligned}
$$

Next, we integrate from t to $t+\tau$:

$$
\begin{aligned}
\int_t^{t+\tau} E_t^P[r_s]\mathrm{d}s &= \int_t^{t+\tau} \left(\left[1 - \kappa_{21}^P \frac{1 - \mathrm{e}^{-\kappa_{22}^P(s-t)}}{\kappa_{22}^P}\right] L_t + \theta_2^P + \mathrm{e}^{-\kappa_{22}^P(s-t)}\left(S_t - \theta_2^P\right) \right. \\
&\quad \left. - \kappa_{23}^P \frac{\mathrm{e}^{-\kappa_{33}^P(s-t)} - \mathrm{e}^{-\kappa_{22}^P(s-t)}}{\kappa_{22}^P - \kappa_{33}^P}\left(C_t - \theta_3^P\right) \right) \mathrm{d}s \\
&= \theta_2^P \tau + \left(1 - \frac{\kappa_{21}^P}{\kappa_{22}^P}\right) \tau L_t + \frac{\kappa_{21}^P}{\kappa_{22}^P} L_t \int_t^{t+\tau} \mathrm{e}^{-\kappa_{22}^P(s-t)}\mathrm{d}s \\
&\quad + \left(S_t - \theta_2^P\right) \int_t^{t+\tau} \mathrm{e}^{-\kappa_{22}^P(s-t)}\mathrm{d}s \\
&\quad - \frac{\kappa_{23}^P}{\kappa_{22}^P - \kappa_{33}^P}\left(C_t - \theta_3^P\right) \int_t^{t+\tau} \left(\mathrm{e}^{-\kappa_{33}^P(s-t)} - \mathrm{e}^{-\kappa_{22}^P(s-t)}\right)\mathrm{d}s \\
&= \theta_2^P \tau + \left(1 - \frac{\kappa_{21}^P}{\kappa_{22}^P}\right) \tau L_t - \frac{\kappa_{21}^P}{\kappa_{22}^P} L_t \left[\frac{1}{\kappa_{22}^P} \mathrm{e}^{-\kappa_{22}^P(s-t)}\right]_t^{t+\tau} \\
&\quad + \left(S_t - \theta_2^P\right) \left[\frac{-1}{\kappa_{22}^P} \mathrm{e}^{-\kappa_{22}^P(s-t)}\right]_t^{t+\tau} \\
&\quad - \frac{\kappa_{23}^P}{\kappa_{22}^P - \kappa_{33}^P}\left(C_t - \theta_3^P\right) \left[\frac{-1}{\kappa_{33}^P} \mathrm{e}^{-\kappa_{33}^P(s-t)} + \frac{1}{\kappa_{22}^P} \mathrm{e}^{-\kappa_{22}^P(s-t)}\right]_t^{t+\tau} \\
&= \theta_2^P \tau + \left(1 - \frac{\kappa_{21}^P}{\kappa_{22}^P}\right) \tau L_t + \frac{\kappa_{21}^P}{\kappa_{22}^P} \frac{1 - \mathrm{e}^{-\kappa_{22}^P \tau}}{\kappa_{22}^P} L_t + \frac{1}{\kappa_{22}^P}\left(S_t - \theta_2^P\right)\left(1 - \mathrm{e}^{-\kappa_{22}^P \tau}\right) \\
&\quad - \frac{\kappa_{23}^P}{\kappa_{22}^P - \kappa_{33}^P}\left(C_t - \theta_3^P\right) \left(\frac{1}{\kappa_{33}^P}\left[1 - \mathrm{e}^{-\kappa_{33}^P \tau}\right] - \frac{1}{\kappa_{22}^P}\left[1 - \mathrm{e}^{-\kappa_{22}^P \tau}\right]\right)
\end{aligned}
$$

The relevant term to go into the term premium formula is

$$\begin{aligned}\frac{1}{\tau}\int_t^{t+\tau} E_t^P[r_s]\mathrm{d}s \;=\; & \theta_2^P + \left(1-\frac{\kappa_{21}^P}{\kappa_{22}^P}\right)L_t + \frac{\kappa_{21}^P}{\kappa_{22}^P}\frac{1-\mathrm{e}^{-\kappa_{22}^P\tau}}{\kappa_{22}^P\tau}L_t + \frac{1-\mathrm{e}^{-\kappa_{22}^P\tau}}{\kappa_{22}^P\tau}\left(S_t-\theta_2^P\right) \\ & -\frac{\kappa_{23}^P}{\kappa_{22}^P-\kappa_{33}^P}\left(\frac{1-\mathrm{e}^{-\kappa_{33}^P\tau}}{\kappa_{33}^P\tau}-\frac{1-\mathrm{e}^{-\kappa_{22}^P\tau}}{\kappa_{22}^P\tau}\right)\left(C_t-\theta_3^P\right)\end{aligned}$$

The final expression for the term premium is then given by

$$\begin{aligned}TP_t(\tau) \;=\; & y_t(\tau) - \frac{1}{\tau}\int_t^{t+\tau} E_t^P[r_s]\mathrm{d}s \\ =\; & L_t + \frac{1-\mathrm{e}^{-\lambda\tau}}{\lambda\tau}S_t + \left(\frac{1-\mathrm{e}^{-\lambda\tau}}{\lambda\tau}-\mathrm{e}^{-\lambda\tau}\right)C_t - \frac{A(\tau)}{\tau} \\ & -\theta_2^P - \left(1-\frac{\kappa_{21}^P}{\kappa_{22}^P}\right)L_t - \frac{\kappa_{21}^P}{\kappa_{22}^P}\frac{1-\mathrm{e}^{-\kappa_{22}^P\tau}}{\kappa_{22}^P\tau}L_t - \frac{1-\mathrm{e}^{-\kappa_{22}^P\tau}}{\kappa_{22}^P\tau}\left(S_t-\theta_2^P\right) \\ & +\frac{\kappa_{23}^P}{\kappa_{22}^P-\kappa_{33}^P}\left(\frac{1-\mathrm{e}^{-\kappa_{33}^P\tau}}{\kappa_{33}^P\tau}-\frac{1-\mathrm{e}^{-\kappa_{22}^P\tau}}{\kappa_{22}^P\tau}\right)\left(C_t-\theta_3^P\right) \\ =\; & \frac{\kappa_{21}^P}{\kappa_{22}^P}\left(1-\frac{1-\mathrm{e}^{-\kappa_{22}^P\tau}}{\kappa_{22}^P\tau}\right)L_t + \left(\frac{1-\mathrm{e}^{-\lambda\tau}}{\lambda\tau}-\frac{1-\mathrm{e}^{-\kappa_{22}^P\tau}}{\kappa_{22}^P\tau}\right)S_t \\ & +\left(\frac{1-\mathrm{e}^{-\lambda\tau}}{\lambda\tau}-\mathrm{e}^{-\lambda\tau}+\frac{\kappa_{23}^P}{\kappa_{22}^P-\kappa_{33}^P}\left[\frac{1-\mathrm{e}^{-\kappa_{33}^P\tau}}{\kappa_{33}^P\tau}-\frac{1-\mathrm{e}^{-\kappa_{22}^P\tau}}{\kappa_{22}^P\tau}\right]\right)C_t \\ & -\left(1-\frac{1-\mathrm{e}^{-\kappa_{22}^P\tau}}{\kappa_{22}^P\tau}\right)\theta_2^P - \frac{\kappa_{23}^P}{\kappa_{22}^P-\kappa_{33}^P}\left(\frac{1-\mathrm{e}^{-\kappa_{33}^P\tau}}{\kappa_{33}^P\tau}-\frac{1-\mathrm{e}^{-\kappa_{22}^P\tau}}{\kappa_{22}^P\tau}\right)\theta_3^P - \frac{A(\tau)}{\tau}\end{aligned}$$

In the B-CR model, $\frac{1}{\tau}\int_t^{t+\tau} E_t^P[r_s]\mathrm{d}s$ is not available in analytical form, instead it has to be approximated by numerically integrating the formula for $E_t^P[r_s]$ provided in Appendix B.